

Octyl-Itaconate Enhances VSV Δ 51 Oncolytic Virotherapy by Multitarget Inhibition of Antiviral and Inflammatory Pathways

Naziia Kurmasheva *et al.*

This PDF file includes:

- Supplementary Figures 1-19
- Supplementary Tables 1-6
- Supplementary Methods (Copies of NMR spectra)

Supplementary Figures 1-19

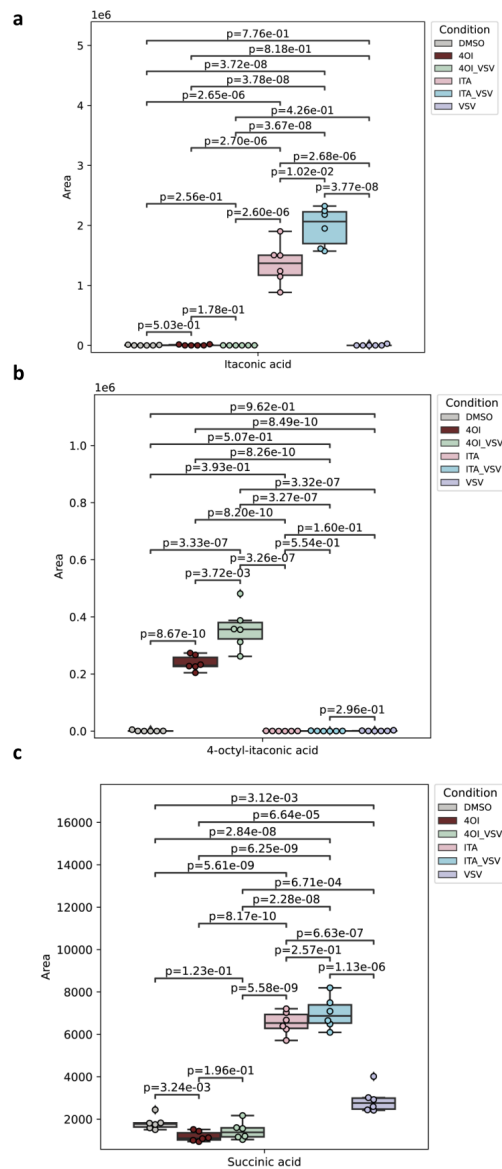


Figure S1. Modulation of metabolites production in 4-OI vs itaconate-treated and VSV Δ 51-infected cancer cells

a-c 786-O cells were either pre-treated with 4-OI (75 μ M) or itaconate (10 mM) for 24 hrs and subsequently infected with VSV Δ 51 (MOI 0.01) for 17 hours. Metabolites were measured by LC mass spectrometry. Data come from one experiment performed in sextuplicate. Data are depicted as: each box shows the interquartile range (IQR) extending between [Q1, Q3], the line inside the box indicates the median value, the “whiskers” extend to points that lie within 1.5 IQRs of Q1 and Q3. Statistics indicate significance by two-tailed Student’s t-test for **a-c**. Source data are provided as a Source Data file.

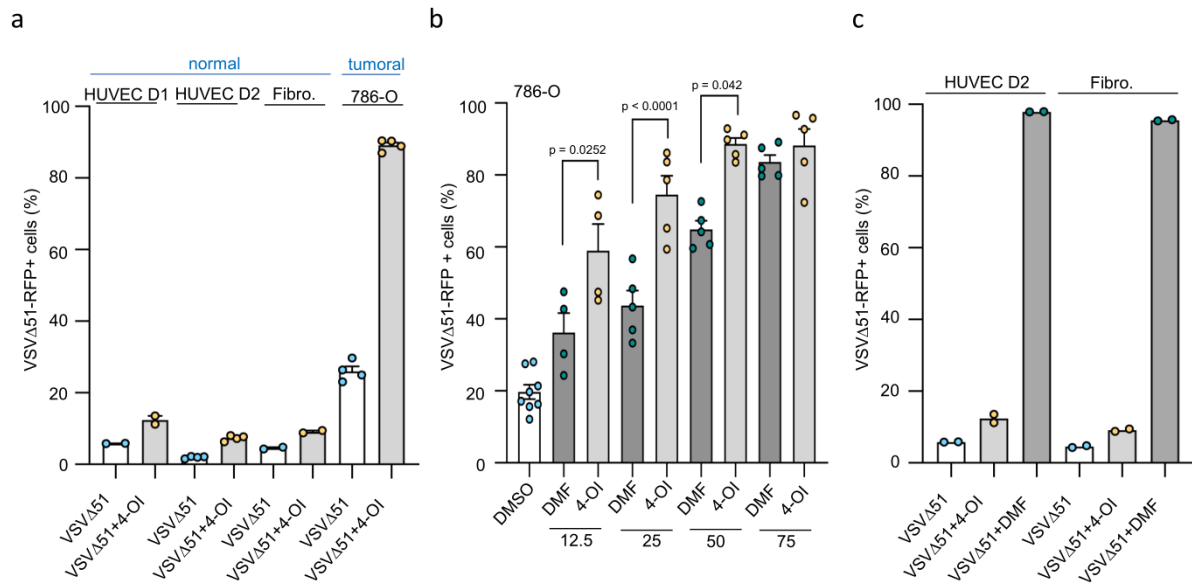


Figure S2. 4-OI outperforms the OV boosting capacity of dimethyl fumarate in vitro and does not enhance VSVΔ51 infection in non-tumoral cells

a Primary HUVECs from two different donors (D1 and D2), primary human fibroblasts and tumoral 786-O cells were pre-treated with 4-OI (125 μM) for 24 hours and subsequently infected with VSVΔ51 (MOI 0.01) for 17 hours. The number of infected RFP+ cells was quantified by flow cytometry.

b 786-O cells were pre-treated with the indicated concentrations of 4-OI or dimethyl fumarate (DMF) for 24 hours and subsequently infected with VSVΔ51 (MOI 0.01) for 17 hours. The number of infected RFP+ cells was quantified by flow cytometry.

c Primary HUVECs from donor 2 (D2), and primary human fibroblasts were pre-treated with 4-OI (125 μM) or DMF (100 μM) for 24 hours and subsequently infected with VSVΔ51 (MOI 0.01) for 17 hours. The number of infected RFP+ cells was quantified by flow cytometry. Data are depicted as means ± SEM from two experiments performed in duplicate in **a** and from two experiments performed in triplicate and quadruplicate in **b**. Data are depicted as means ± SEM from one experiment performed in duplicate in **c**. Statistics indicate significance by one-way ANOVA for **b**. Source data are provided as a Source Data file.

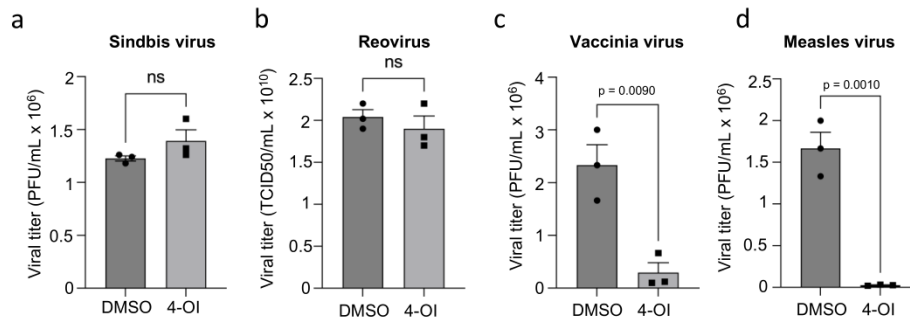
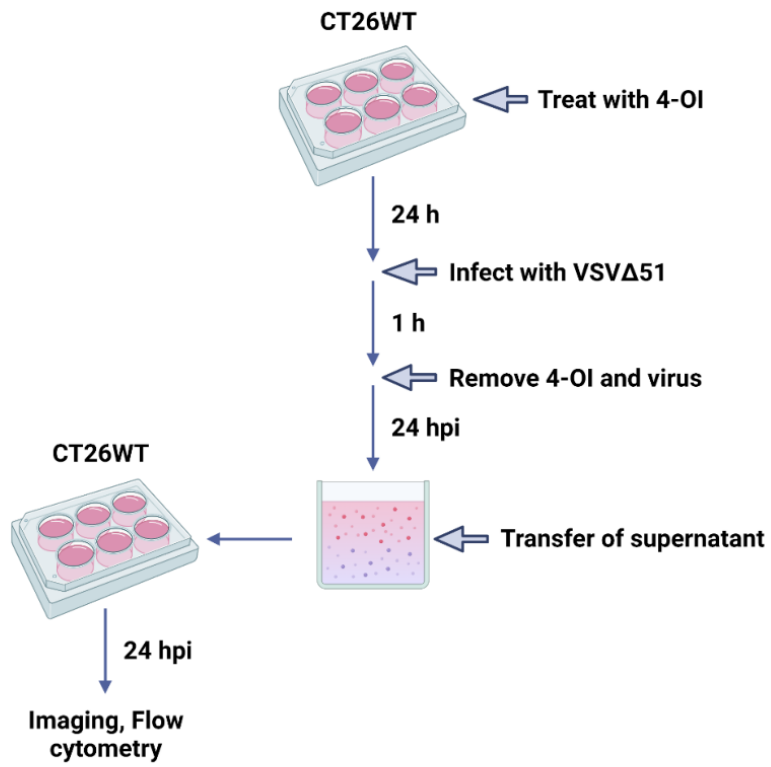


Figure S3. 4-OI restricts infection of oncolytic Vaccinia and Measles in cancer cells and has no effect on Sindbis and Reovirus infection

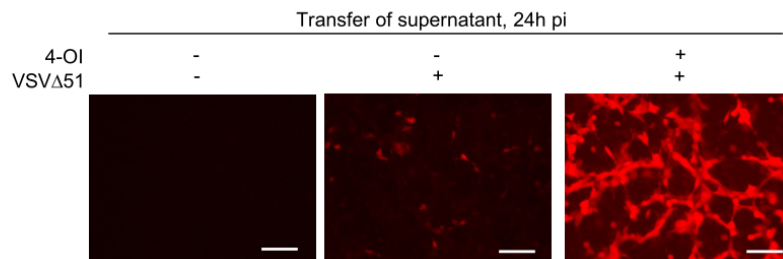
a 786-O cells were pre-treated with 4-OI (100 μ M) for 24 hours and subsequently infected with Sindbis virus (MOI 10) for 48 hrs. Viral titers were determined in the supernatants of infected cells by plaque assay.

b-d PANC1 cells were pre-treated with 4-OI (125 μ M) for 24 hours and subsequently infected with Reovirus (10^6 TCID50/ml), vaccinia virus (MOI 0.01) and Measles virus (MOI 0.1) for 48 hrs. Viral titers were determined in the supernatants of infected cells by plaque assay or TCID50. Data are depicted as means \pm SEM from one experiment performed in triplicate in **a-d**. Statistics indicate significance by two-tailed Student's t-test for **a-d**. Source data are provided as a Source Data file.

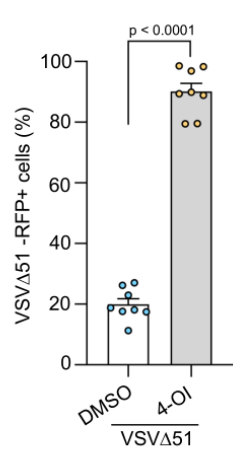
a



b



c



d

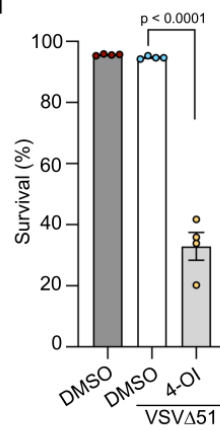


Figure on previous page

Figure S4. Transfer of supernatants from virus-infected and 4-OI-treated cells can promote OV infection in bystander untouched cancer cells

a Schematic representing the layout of the supernatant transfer experiment. CT26WT cells were treated with 4-OI (125 μ M) for 24hrs following 1h incubation with VSV Δ 51 (MOI 0.01). The supernatants containing virus were washed off and replaced by fresh medium (not containing virus or 4-OI). 24 hrs later these media were transferred to freshly plated CT26WT cells for another 24 hrs. Infectivity and survival were assessed 24 hrs after incubation with the supernatants.

b-d Supernatants containing virus from 4-OI- or DMSO-stimulated CT26WT cells was transferred to bystander untouched cells for 24 hours. Infectivity was assessed by fluorescence microscopy (**b**) (Scale bars, 100 μ m) or flow cytometry of RFP⁺ cells (**c**).

Data are depicted as means \pm SEM from two experiments performed in quadruplicate in **c** and from two experiments performed in duplicate in **d**. Pictures in are representative of one experiment performed three times in **c**. Statistics indicate significance by two-tailed Student's t-test for **c** and one-way ANOVA in **d**. Panel **a** has been created using BioRender.com. Source data are provided as a Source Data file.

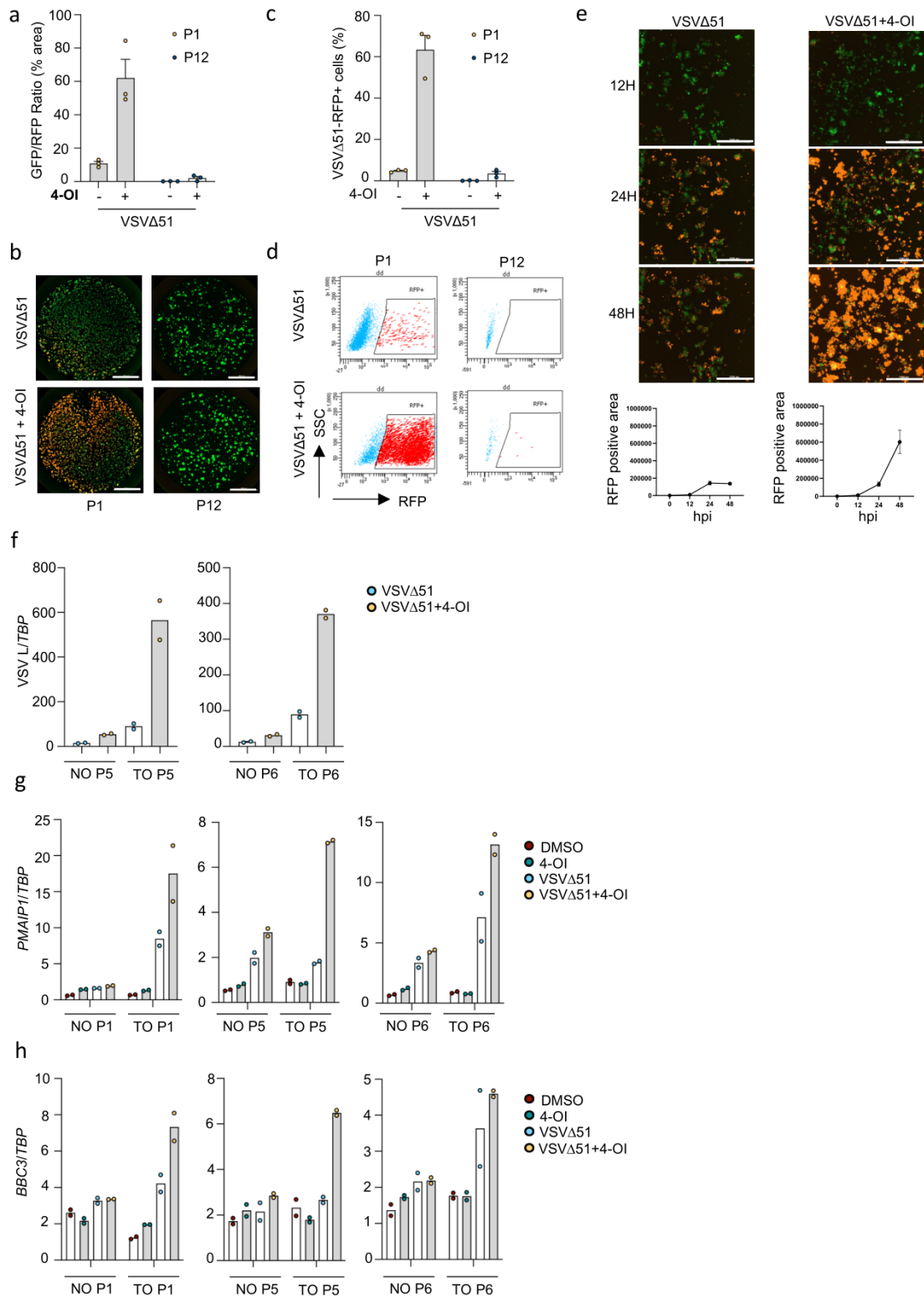


Figure on previous page

Figure S5. 4-OI increases oncolytic infectivity and killing by VSV Δ 51 in 3D patient-derived colon cancer tumoroids

a-b Fluorescence area quantification (48-well plate) to evaluate the infectivity of VSV Δ 51-RFP infection (1×10^6 pfu/well) solely, and in combination with 4-OI (125 μ M), within colon cancer organoids derived from two patients (P1 and P12) 48 hours post infection. To assess for total organoid area, organoids were either transduced with GFP or stained with calcein green. Scale bars, 3000 μ m.

c-d Flow cytometry counts of infected RFP-positive cells from enzymatically digested colon tumoroids in patient 1 and 12 (P1 and P12) at 48 hours post infection with VSV Δ 51 infection (1×10^6 pfu/well) in the presence or not of 4-OI (125 μ M).

e RFP area signal from VSV Δ 51-RFP (1×10^6 pfu/well) to evaluate virus infection solely or in combination with 4-OI (125 μ M), within colon cancer organoids derived from one patient (P1) at different time post infection. Scale bars, 1000 μ m.

f qPCR analysis of VSV L gene expression within colon NO (normal) and TO (tumoral) organoids from patient 5 (P5) and patient 6 (P6), one day post infection with VSV Δ 51 (1×10^6 pfu/well) in the presence or not of 4-OI (125 μ M)

g-h qPCR analysis of NOXA (*PMAIP1*) (g) and PUMA (*BBC3*) (h) gene expression within colon NO (normal) and TO (tumoral) organoids from different patients (P1, P5 and P6), one day post infection with VSV Δ 51 (1×10^6 pfu/well) in the presence or not of 4-OI (125 μ M). Data are depicted as means \pm SEM from one experiment performed in biological triplicates from two patients in **a,b**, from one experiment performed in biological triplicates from two patients in **c-d**, from one experiment on one patient in **e**, from one experiment performed in biological duplicates in two to three patients in **f-h**. Source data are provided as a Source Data file.

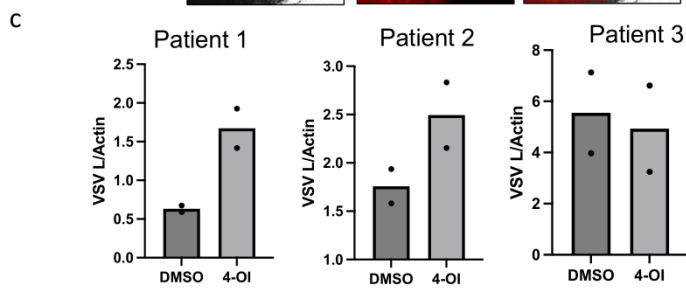
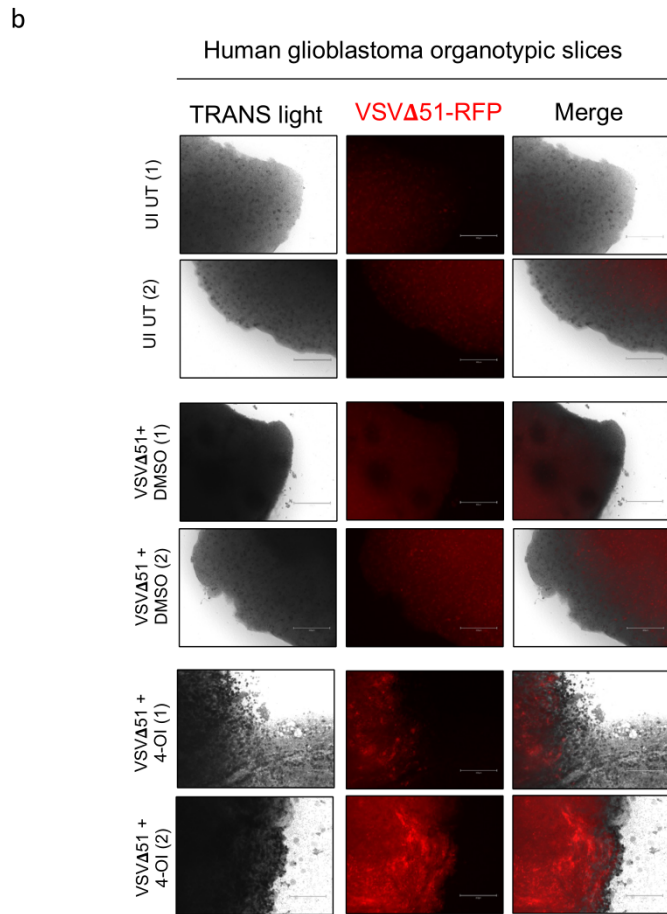
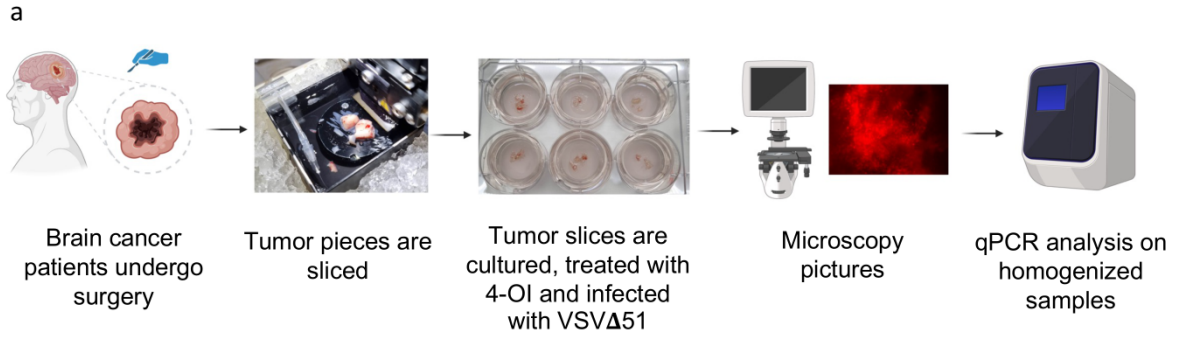


Figure on previous page

Figure S6. 4-OI increases VSV Δ 51 in patient-derived organotypic brain cancer slices

a Schematic highlighting the procedure of the experiment.

b Organotypic glioblastoma slices were infected with VSV Δ 51-RFP (4×10^6 PFU) in the presence of 4-OI (125 μ M) for 20 hrs. Infectivity of the slices was assessed by fluorescence imaging. Scale bars, 300 μ m.

c qPCR analysis of VSV L gene expression within the tumor slices from four patients; 20 hours post infection with VSV Δ 51 (4×10^6 PFU) in the presence or not of 4-OI (125 μ M) (P1), 40 hours post infection with VSV Δ 51 (8×10^6 PFU) in the presence or not of 4-OI (125 μ M) (P2-P3). Data are from one experiment performed on three different patients (**Table S2**). For the qPCR, experiments were done in biological duplicates and display the means. Panel **a** has been created using BioRender.com. Source data are provided as a Source Data file.

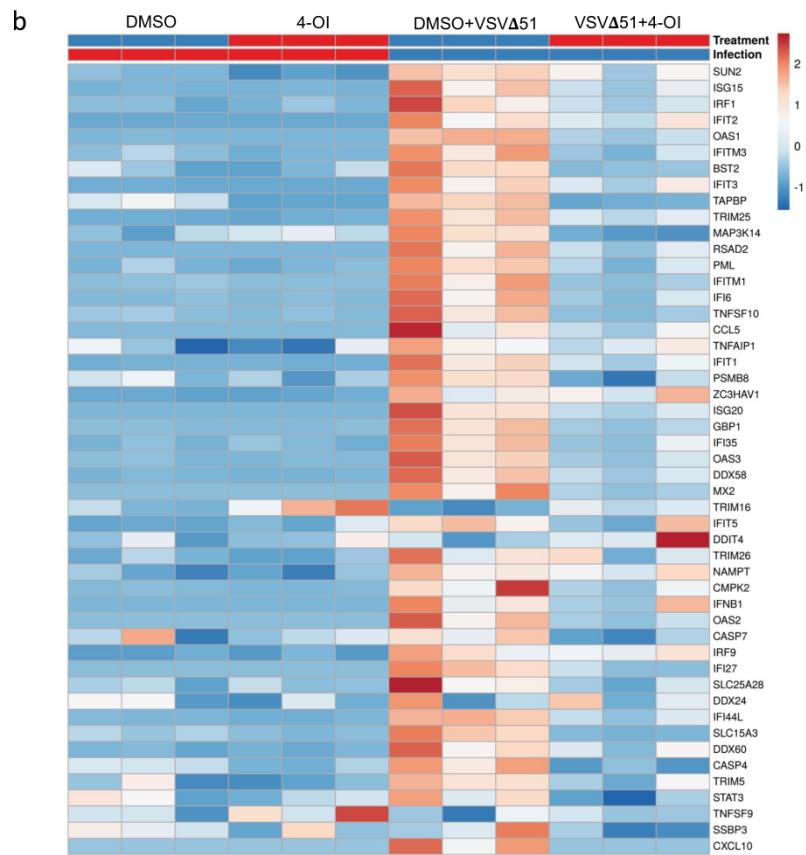
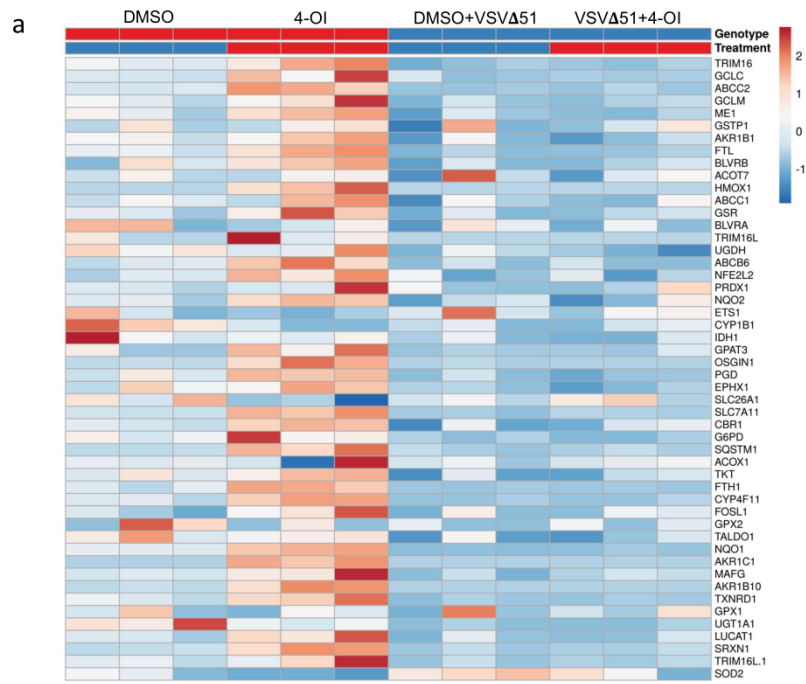


Figure on previous page

Figure S7. Heatmap of differentially expressed antiviral and NRF2-regulated genes in 4-OI-stimulated NRF2 KO cancer cells

a-b 786-O cells were pre-treated with 4-OI (75 μ M) for 24 hours and subsequently infected with VSV Δ 51 (MOI 0.01) for 17 hours. RNA was analyzed using RNA sequencing. Heat map showing the expression of differentially expressed NRF2-regulated genes (**a**) and interferon stimulated genes (ISGs) (**b**) across all experimental conditions. Data are from one experiment performed in triplicate.

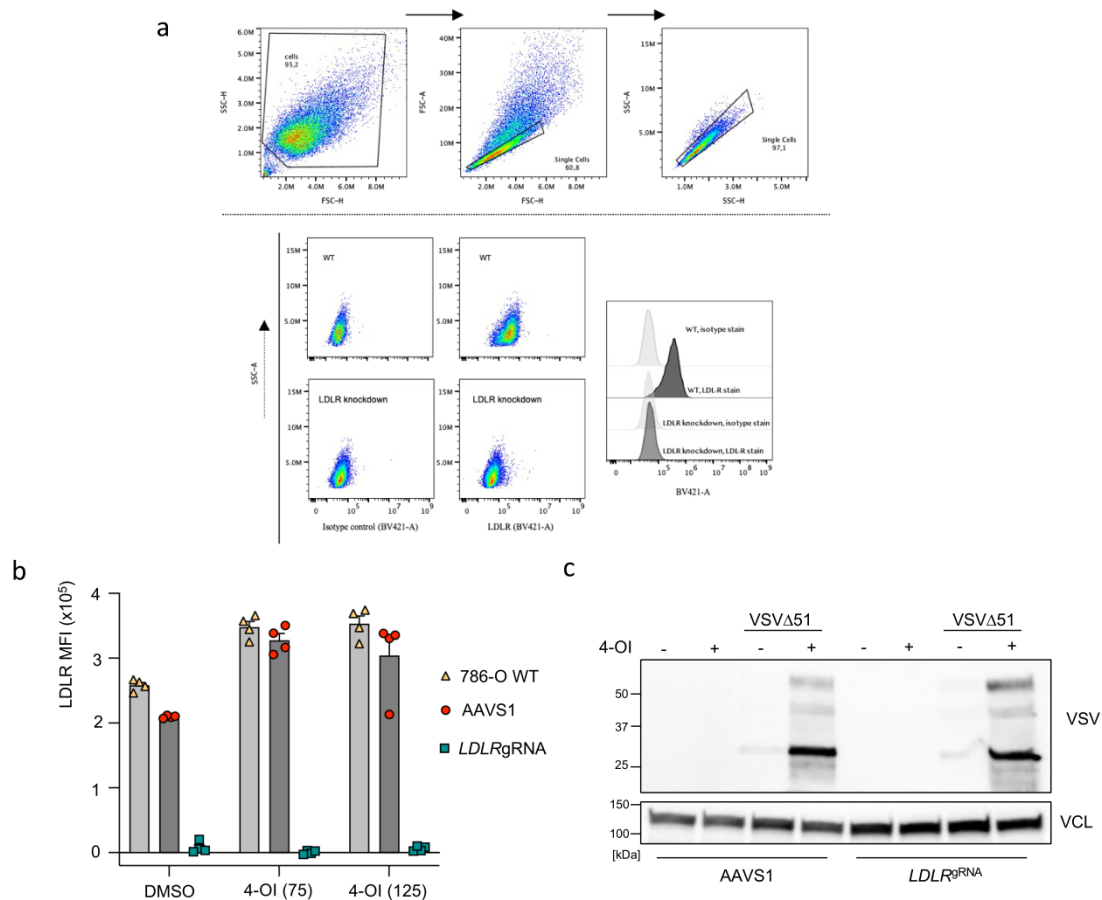


Figure S8. 4-OI does not promote OV infectivity in cancer cells via the modulation of LDL Receptor Surface Levels

a Representative flow cytometry plots showing the gating strategy used to determine the LDLR expression. Total cells were selected using SSC-H/FSC-H gating, followed by FSC-A/FSC-H and SSC-A/SSC-H to select for single cells, which were used to measure the BV421 fluorescence upon staining with LDLR-BV421 antibody or the respective BV421-conjugated isotype control.

b 786-O cells were transiently KO for LDL Receptor (LDLR) (*LDLR*^{gRNA}) using CRISPR/Cas9 gene editing, treated with a control gRNA sequence (AAVS1) or simply electroporated (786-O WT). Following CRISPR/Cas9 gene editing, cells were treated with 4-OI (75 or 125 μ M) for 24 hours and LDLR surface levels was assessed by flow cytometry.

c 786-O cells transiently KO for LDL Receptor (LDLR) (*LDLR*^{gRNA}) using CRISPR/Cas9 gene editing were pre-treated with 4-OI (75 μ M) for 24 hours and subsequently infected with VSV Δ 51 (MOI 0.01) for 17 hours. Western blot was performed on cell lysates for VSV proteins. Vinculin (VCL) was used as a housekeeping control. Data are depicted as means \pm SEM from two experiments performed in duplicate in **a-b**. WB is representative of one experiment performed twice in **c**. Source data are provided as a Source Data file.

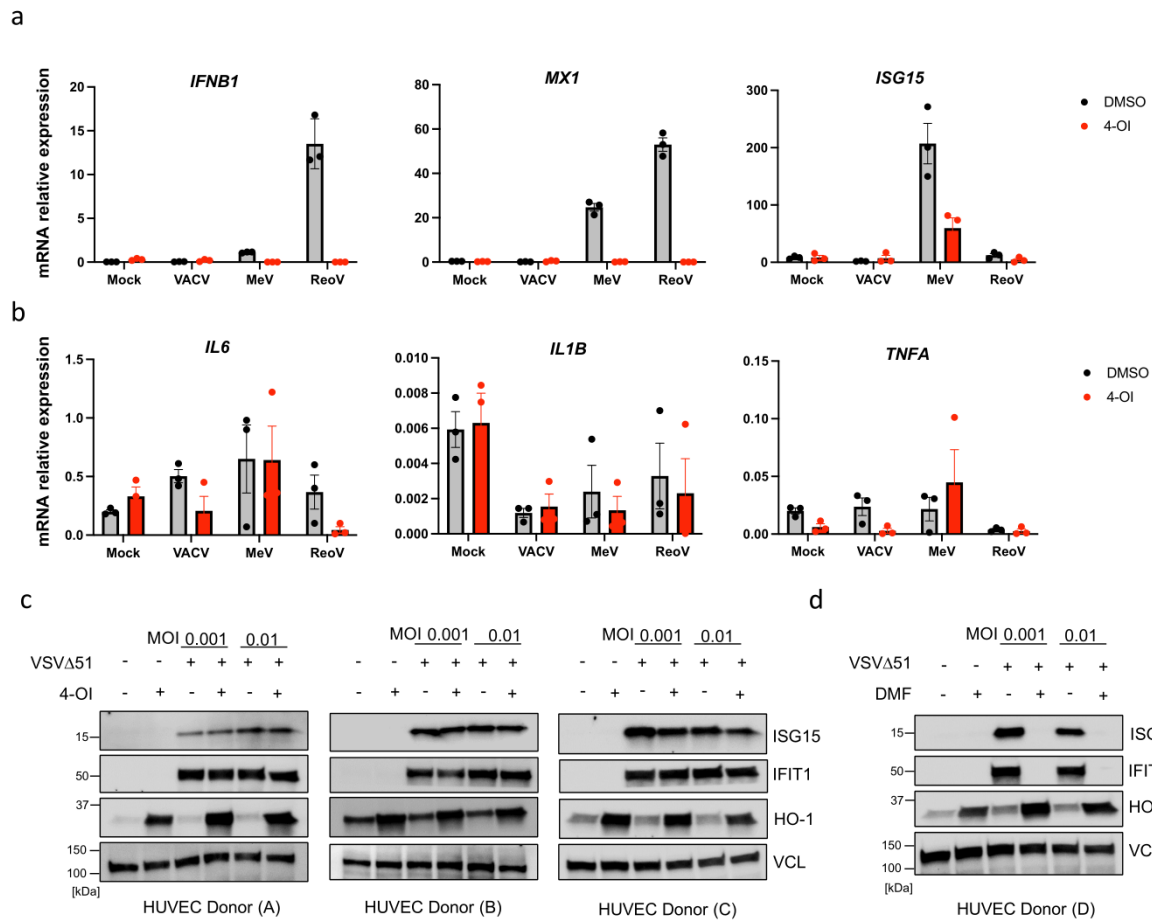


Figure S9. Modulation of antiviral immune responses by 4-OI in tumoral and normal cells

a-b PANC1 cells were pre-treated with 4-OI (125 μ M) for 24 hours and subsequently infected with Reovirus (10^6 TCID₅₀/ml), vaccinia virus (MOI 0.01) and Measles virus (MOI 0.1) for 48 hrs. Antiviral and inflammatory gene levels were determined by qPCR.

c-d Primary HUVECs from four different donors (Donor A to Donor D) were pre-treated with 4-OI (125 μ M) (c) or DMF (100 μ M) (d) for 24 hours and subsequently infected with VSV Δ 51 (MOI 0.001 or MOI 0.01) for 17 hours. Antiviral immune responses were assessed by immunoblotting of IFIT1 and ISG15. HO-1 served as a positive control of NRF2 induction and VCL was using as an invariant loading control. Data are depicted as means \pm SEM from one experiment performed in triplicates in **a-b**. Vertical stacks of bands are not derived from the same membrane in **c** and **d**. Source data are provided as a Source Data file.

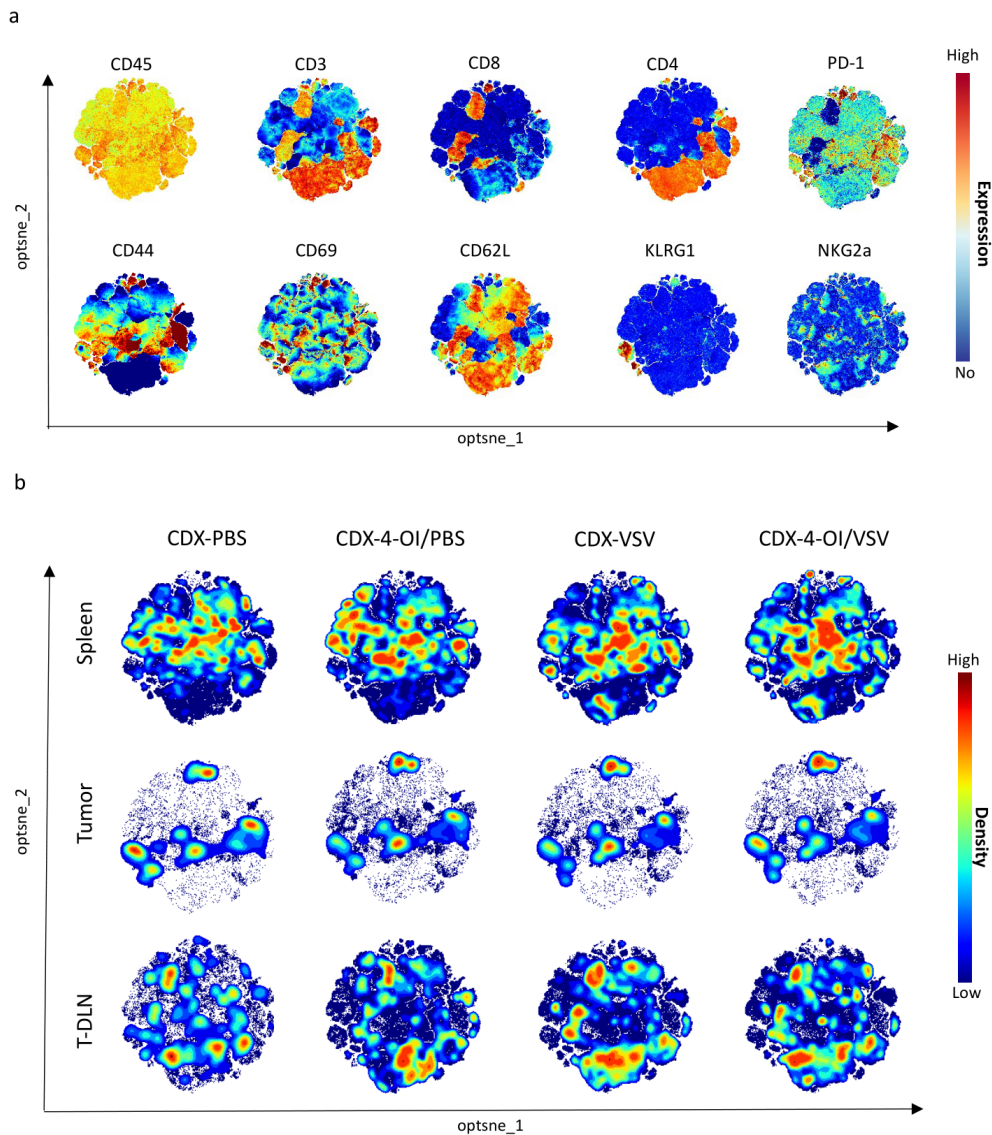


Figure S10. 4-OI and/or VSVA51 does not affect the T-cell landscape within the tumor and lymphoid organs

Flow cytometry data of single cell suspensions isolated from tumor, spleen or tumor-draining lymph node (T-DLN) isolated five days after the last VSVA51 injection. Data was analyzed using OMIQ software.

a Expression intensity profile of T-cell markers on clustered live, CD45⁺ gated samples of all treatment groups and organs (n=57) to distinguish regional expression of single T-cell markers in clusters. Relative expression is indicated by color where red indicates high expression and blue represents no expression within the cluster.

b OptSNE cluster plots of live, CD45⁺ gated samples displayed per organ and treatment group (n=3 mice in CDX-PBS group; n=5 mice in CDX-4-OI/PBS group, n=6 mice in CDX-VSV, and n=6 mice in CDX-4-OI/VSV groups). Cell density is indicated by color where red indicates high density and blue indicates low density within the cluster. 3 individual samples were lost during acquisition: 1 spleen sample in CDX-4-OI/VSV group (n=5), 1 tumor sample in CDX/VSV group (n=5), and 1 T-DLN sample in CDX/VSV group (n=5).

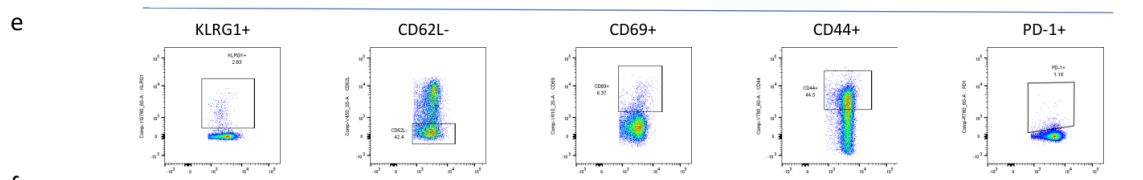
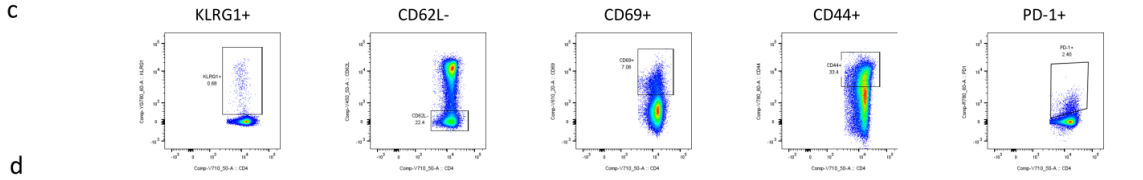
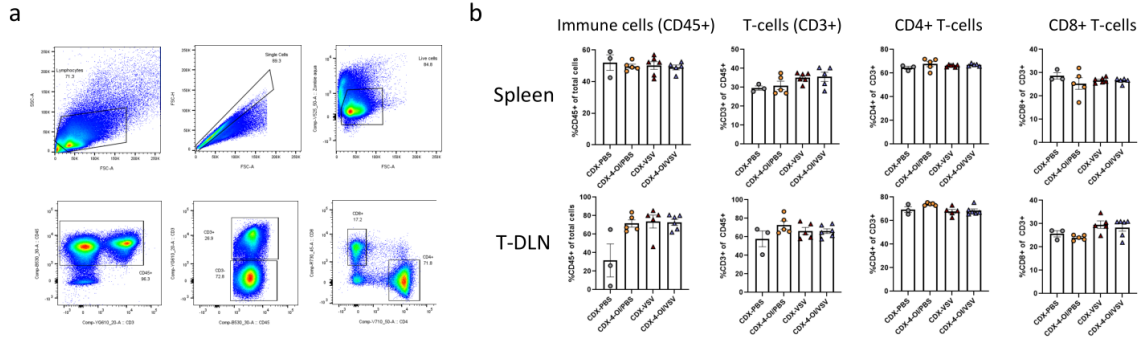


Figure on previous page

Figure S11. 4-OI and/or VSV Δ 51 do not affect T-cell density and phenotype in tumor and lymphoid organs

Flow cytometry analysis of single cell suspensions isolated from tumor, spleen or tumor-draining lymph node (T-DLN) five days after the last VSV Δ 51 injection. Data was analyzed using FlowJo software.

a Representative gating strategy for T-cell populations showed for spleen starting from total cells.

b Mean percentage of indicated T-cell population compared between treatment groups (n=3-6 animals per group). Each dot represents one mouse. n=3 mice in CDX-PBS group; n=5 mice in CDX-4-OI/PBS group, n=6 mice in CDX-VSV, and n=6 mice in CDX-4-OI/VSV groups. 3 individual samples were lost during acquisition: 1 spleen sample in CDX-4-OI/VSV group (n=5), 1 tumor sample in CDX/VSV group (n=5), and 1 T-DLN sample in CDX/VSV group (n=5).

c Representative gating strategy for activation markers on CD4⁺ T-cells showed for spleen.

d Mean percentage of CD4⁺ T-cells expressing different activation markers in spleen, T-DLN and tumor, compared between treatment groups (n=3-6 animals per group).

e Representative gating strategy for activation markers on CD8⁺ T-cells showed for spleen.

f Mean percentage of CD8⁺ T-cells expressing different activation markers in spleen, T-DLN and tumor, compared between treatment groups (n=3-6 animals per group).

P-value is calculated with one-way ANOVA followed by Šídák's multiple comparisons test. No difference found, unless P-value indicated. Source data are provided as a Source Data file.

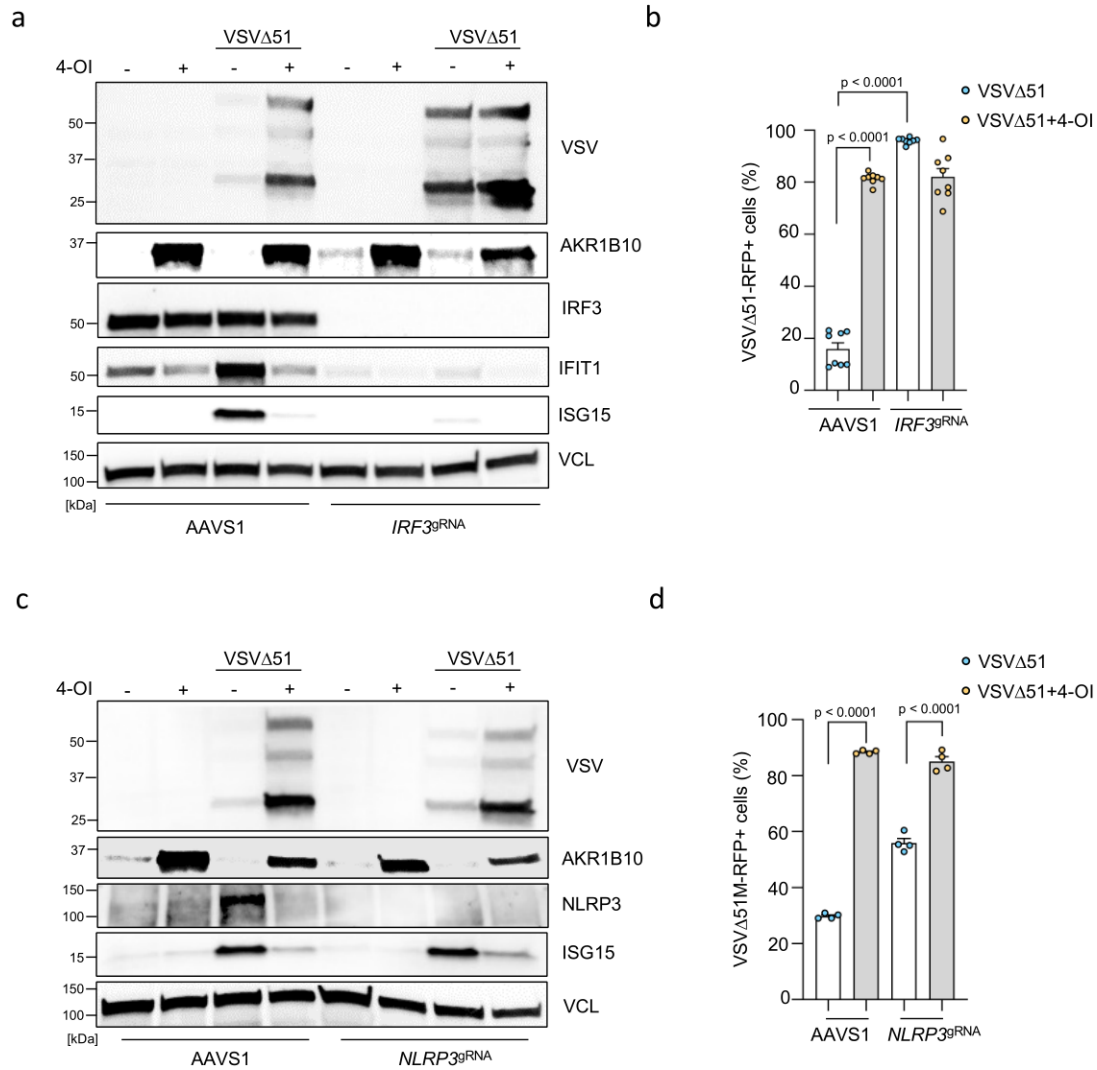


Figure S12. 4-OI does not promote OV infectivity in cancer cells via the alkylation of NLRP3

a-b 786-O cells transiently KO for IRF3 (*IRF3^{gRNA}*) using CRISPR/Cas9 gene editing were pre-treated with 4-OI (75 μ M) for 24 hours and subsequently infected with VSVΔ51 (MOI 0.01) for 17 hours. Western blot was performed on cell lysates for VSV proteins and antiviral markers (a). Vinculin (VCL) was used as a housekeeping control. The number of infected RFP+ cells was quantified by flow cytometry (b).

c-d 786-O cells transiently KO for NLRP3 (*NLRP3^{gRNA}*) using CRISPR/Cas9 gene editing were pre-treated with 4-OI (75 μ M) for 24 hours and subsequently infected with VSVΔ51 (MOI 0.01) for 17 hours. Western blot was performed on cell lysates for VSV proteins and antiviral markers (c). Vinculin (VCL) was used as a housekeeping control. The number of infected RFP+ cells was quantified by flow cytometry (d).

Data are depicted as means \pm SEM from two experiments performed in quadruplicate in **a** and duplicate in **b**. WB is representative of one experiment performed twice in **a** and **b**. Statistics indicate significance by one-way ANOVA in **b** and **d**. Vertical stacks of bands are not derived from the same membrane in **a** and **c**. Source data are provided as a Source Data file.

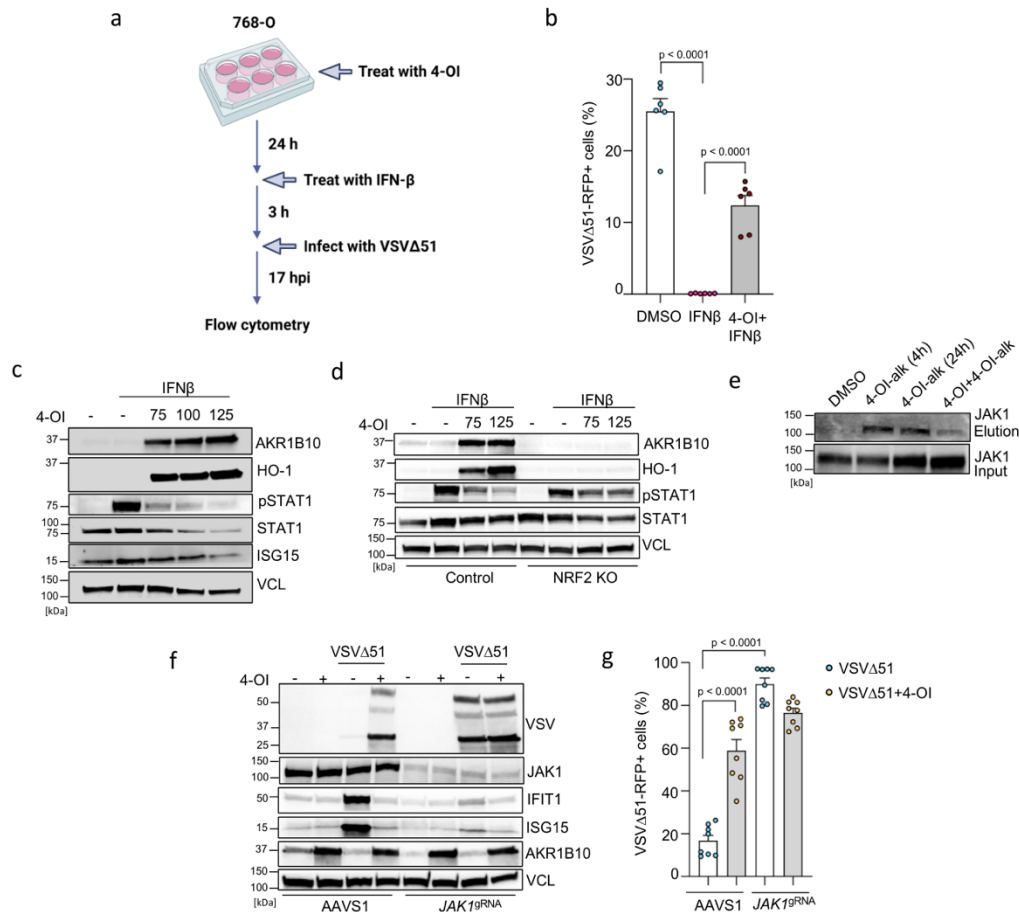


Figure S13. 4-OI enhances VSVA51 infectivity in cancer cell via the impairment of type I IFN signaling through JAK1 direct modification

a-b 768-O cells were treated with 4-OI (75 μ M) for 24 hours prior to IFN β stimulation (200 U/mL) for 3 hours. Cells were subsequently infected with VSVA51 (MOI 0.01) for 17 hours (a) and infectivity was assessed by flow cytometry of infected RFP+ cells.

c-d 768-O cells (c) or control and NRF2 KO 768-O cells (d) were treated with 4-OI at the indicated concentrations for 24 hours prior to IFN β stimulation (250 U/mL) for 30min. Cell lysates were immunoblotted for antiviral proteins and NRF2-related markers. Vinculin (VCL) was used as the invariant housekeeping control.

e 768-O cells were treated with 75 μ M of alkynated 4-OI (4-OI-alk) for 4 or 24 hours in the presence or not of 4-OI (75 μ M). The samples before and after enrichment were analyzed by anti-JAK1 immunoblotting.

f-g 768-O cells transiently KO for JAK1 (*JAK1*^{gRNA}) using CRISPR/Cas9 gene editing were pre-treated with 4-OI (75 μ M) for 24 hours and subsequently infected with VSVA51 (MOI 0.01) for 17 hours. Western blot was performed on cell lysates for VSV proteins and antiviral markers. Vinculin (VCL) was used as a housekeeping control (f). The number of infected RFP+ cells was quantified by flow cytometry (g).

Data are depicted as means \pm SEM from two experiments performed in triplicate in **b**. WB is representative of one experiment performed twice in **c-f**. Data are depicted as means \pm SEM from two experiments performed in quadruplicate in **g**. Statistics indicate significance by one-way ANOVA in **b** and **g**. Vertical stacks of bands are not derived from the same membrane in **c**, **d** and **f**. Source data are provided as a Source Data file.

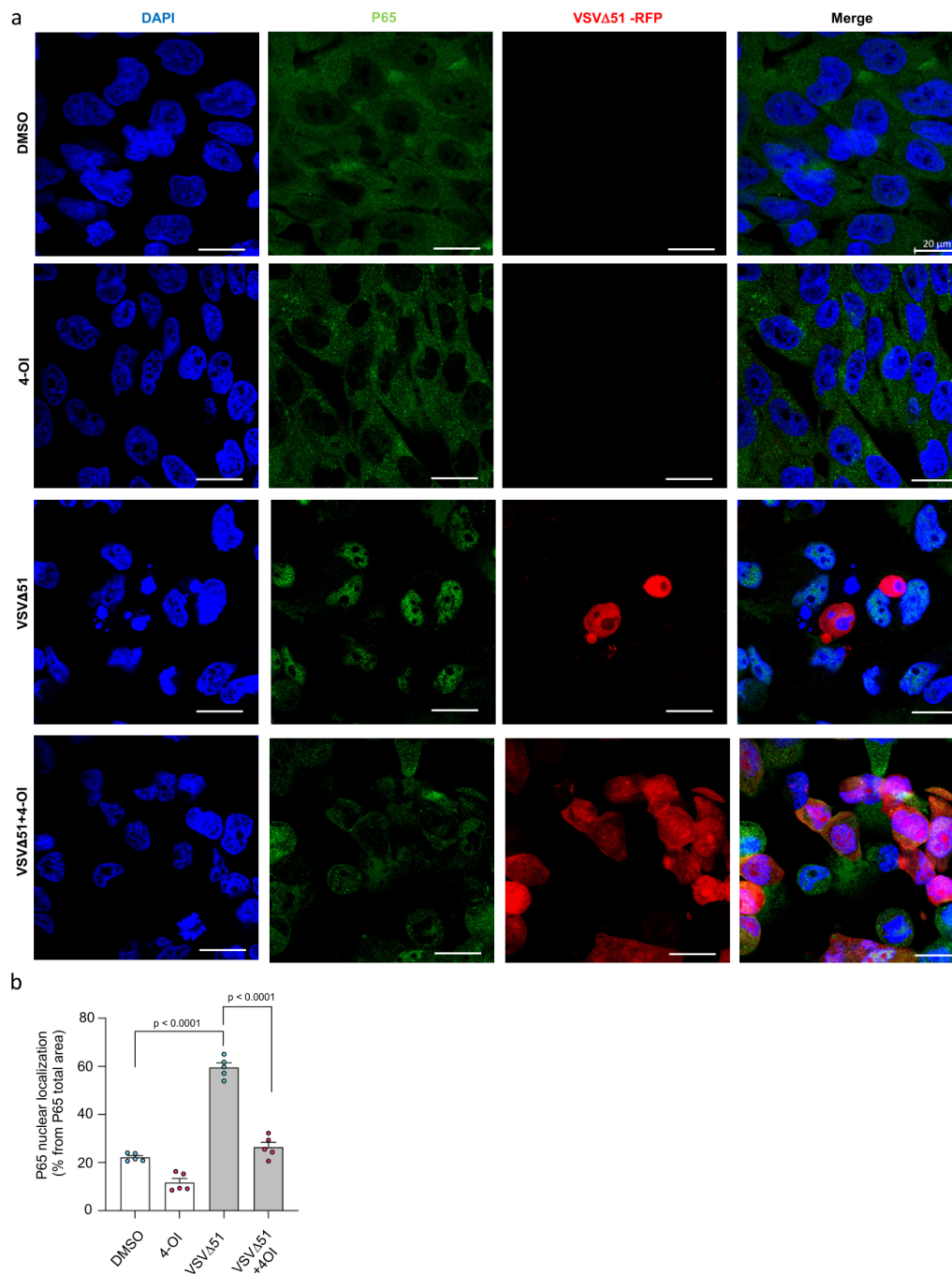


Figure S14. 4-OI prevents the nuclear translocation of RELA upon VSVΔ51 infection

a 786-O cells were pre-treated with 4-OI (75 μ M) for 24 hours and subsequently infected with VSVΔ51 (MOI 0.01) for 17 hours. NF- κ B p65 (RELA) nuclear translocation was assessed by fluorescence microscopy. Nuclei are stained with DAPI. Scale bars, 20 μ m.

b p65 area within nuclear fraction was quantified using Image J software.

The data are representative of one experiment which has been repeated twice in **a**. Data are depicted as means \pm SEM from one experiment performed in five replicates in **b**. Statistics indicate significance by one-way ANOVA in **b**. Source data are provided as a Source Data file.

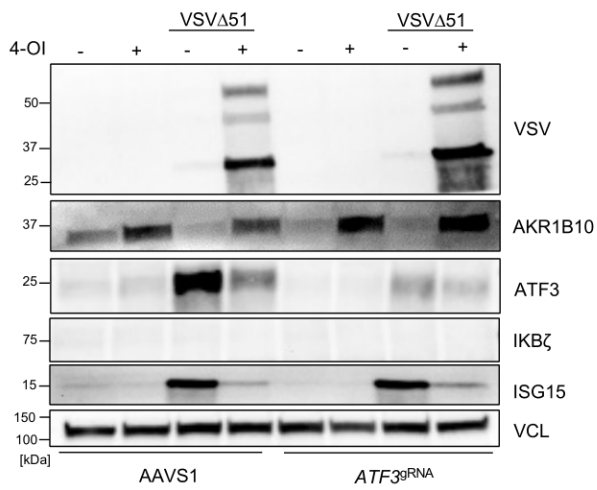
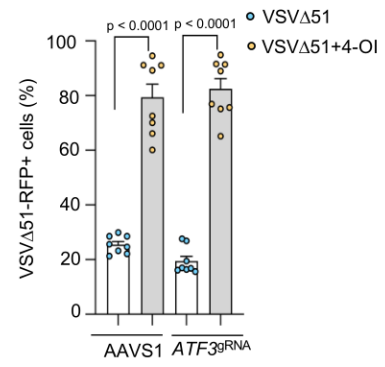
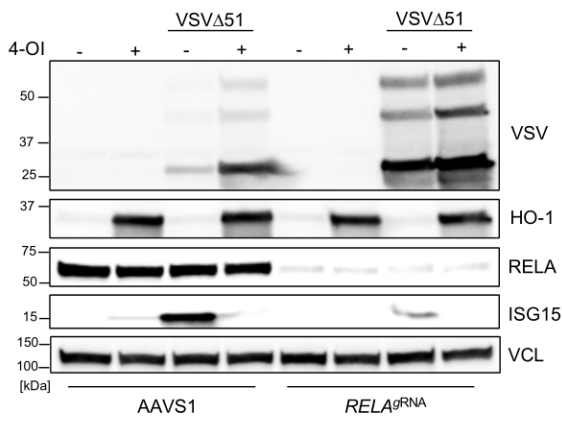
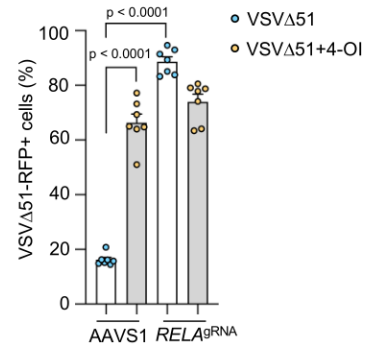
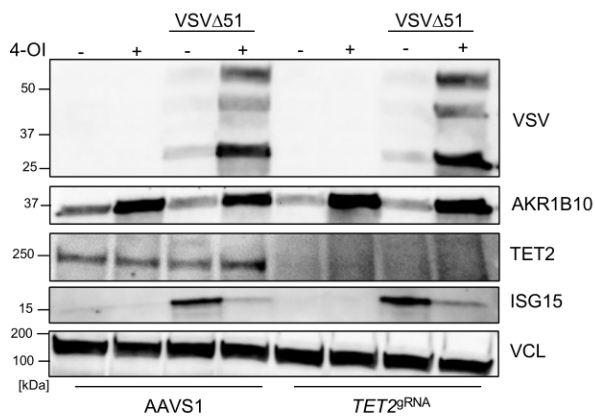
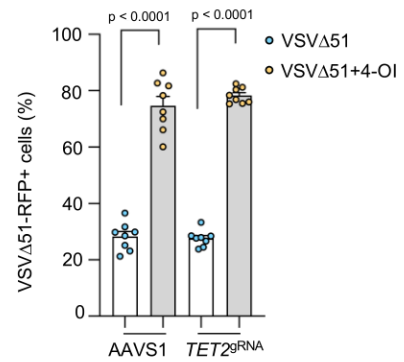
a**b****c****d****e****f**

Figure on previous page

Figure S15. 4-OI does not promote OV infectivity in cancer cells via the alkylation of TET2 or the modulation of the ATF3-IKb ζ axis

a-b 786-O cells transiently KO for ATF3 (*ATF3^{gRNA}*) using CRISPR/Cas9 gene editing were pre-treated with 4-OI (75 μ M) for 24 hours and subsequently infected with VSV Δ 51 (MOI 0.01) for 17 hours. Western blot was performed on cell lysates for VSV proteins and antiviral markers (a). Vinculin (VCL) was used as a housekeeping control. The number of infected RFP+ cells was quantified by flow cytometry (b).

c-d 786-O cells transiently KO for p65/RELA (*RELA^{gRNA}*) using CRISPR/Cas9 gene editing were pre-treated with 4-OI (75 μ M) for 24 hours and subsequently infected with VSV Δ 51 (MOI 0.01) for 17 hours. Western blot was performed on cell lysates for VSV proteins and antiviral markers (c). Vinculin (VCL) was used as a housekeeping control. The number of infected RFP+ cells was quantified by flow cytometry (d).

e-f 786-O cells transiently KO for TET2 (*TET2^{gRNA}*) using CRISPR/Cas9 gene editing were pre-treated with 4-OI (75 μ M) for 24 hours and subsequently infected with VSV Δ 51 (MOI 0.01) for 17 hours. Western blot was performed on cell lysates for VSV proteins and antiviral markers (e). Vinculin (VCL) was used as a housekeeping control. The number of infected RFP+ cells was quantified by flow cytometry (f).

Data are depicted as means \pm SEM from two experiments performed in quadruplicate in **b**, from two experiments in triplicate and quadruplicate in **d**, from two experiments in quadruplicate in **f**. WB is representative of one experiment performed twice in **a**, **c** and **e**. Statistics indicate significance by one-way ANOVA in **b**, **d** and **f**. Vertical stacks of bands are not derived from the same membrane in **a**, **c** and **e**. Source data are provided as a Source Data file.

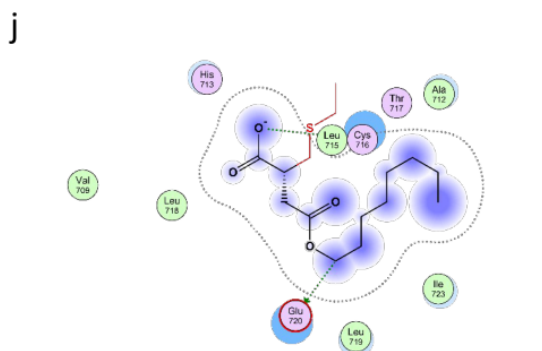
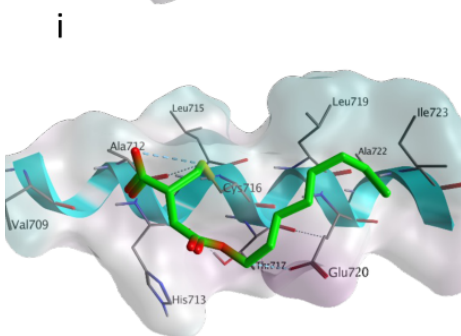
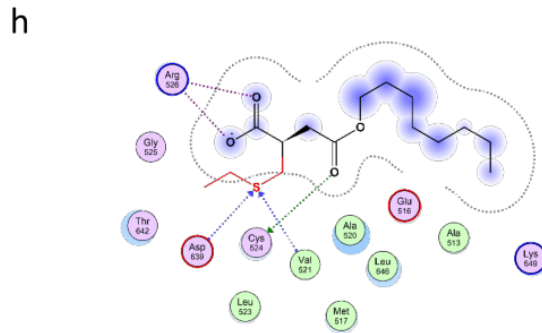
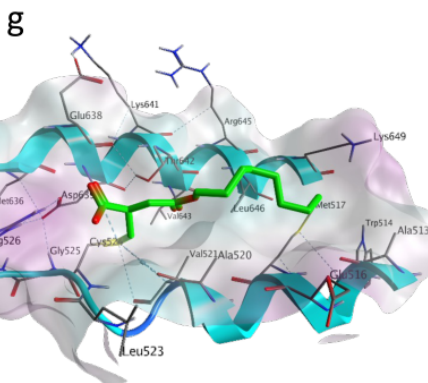
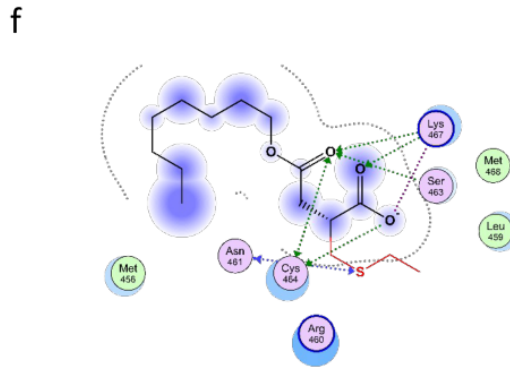
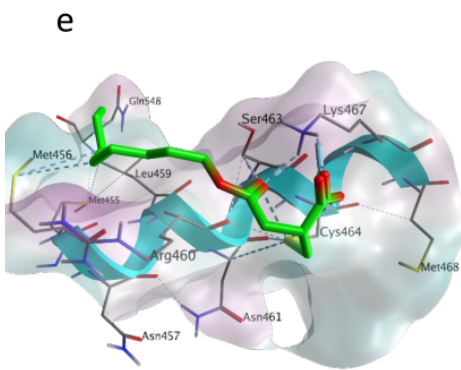
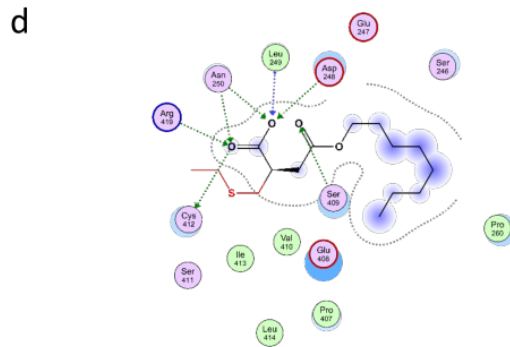
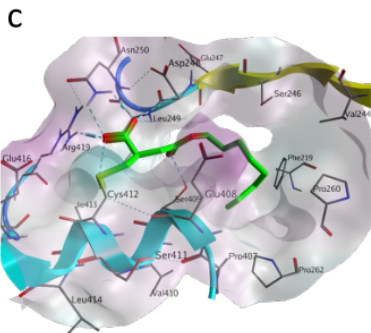
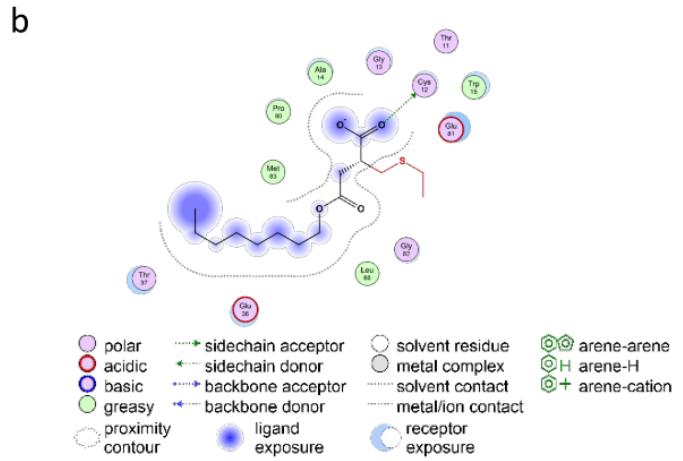
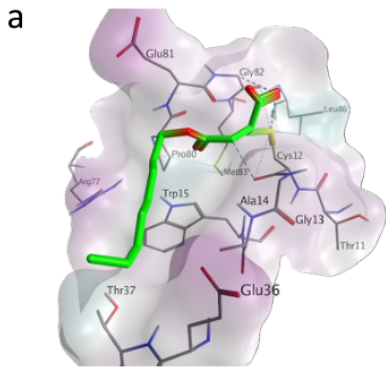


Figure on previous page

Figure S16. Potential covalent binding modes of 4-OI to cysteine residues in human IKK β
a-j Potential covalent binding modes of 4-OI (green) targeting Cys12 (a), Cys412 (c), Cys464 (e), Cys524 (g) and Cys716 (i) in the human IKK β . The corresponding 2D ligand–protein interactions are displayed in (b), (d), (f), (g) and (j), respectively. Lipophilicity protein surface: lipophilic (cyan), hydrophilic (violet), neutral (white), α -helices (cyan), β -sheets (yellow), loops (cyan).

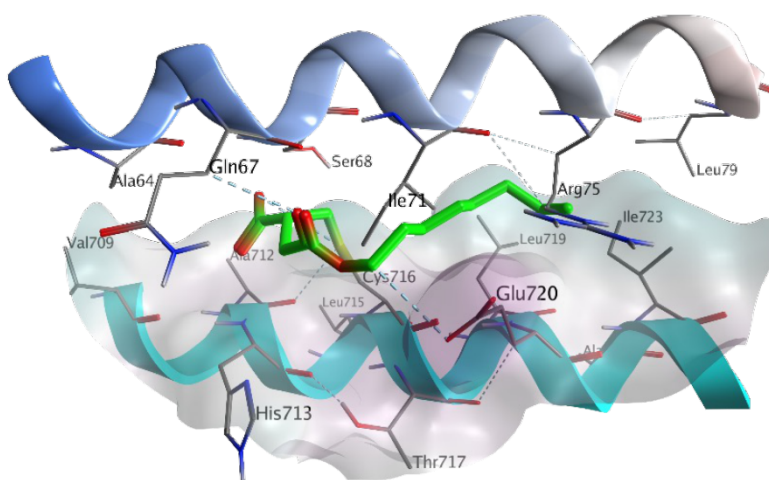


Figure S17. Modelling of 4-OI binding to Cys716 and interaction with NEMO

Overlay of Cys716-bound 4-OI (green) and the α -helix of NEMO (blue) showing steric interactions of the 4-OI octyl moiety with Gln67, Ser68, Ile71 and Arg75 of NEMO. Lipophilicity protein surface: lipophilic (cyan), hydrophilic (violet), neutral (white), α -helices (cyan), β -sheets (yellow), loops (cyan).

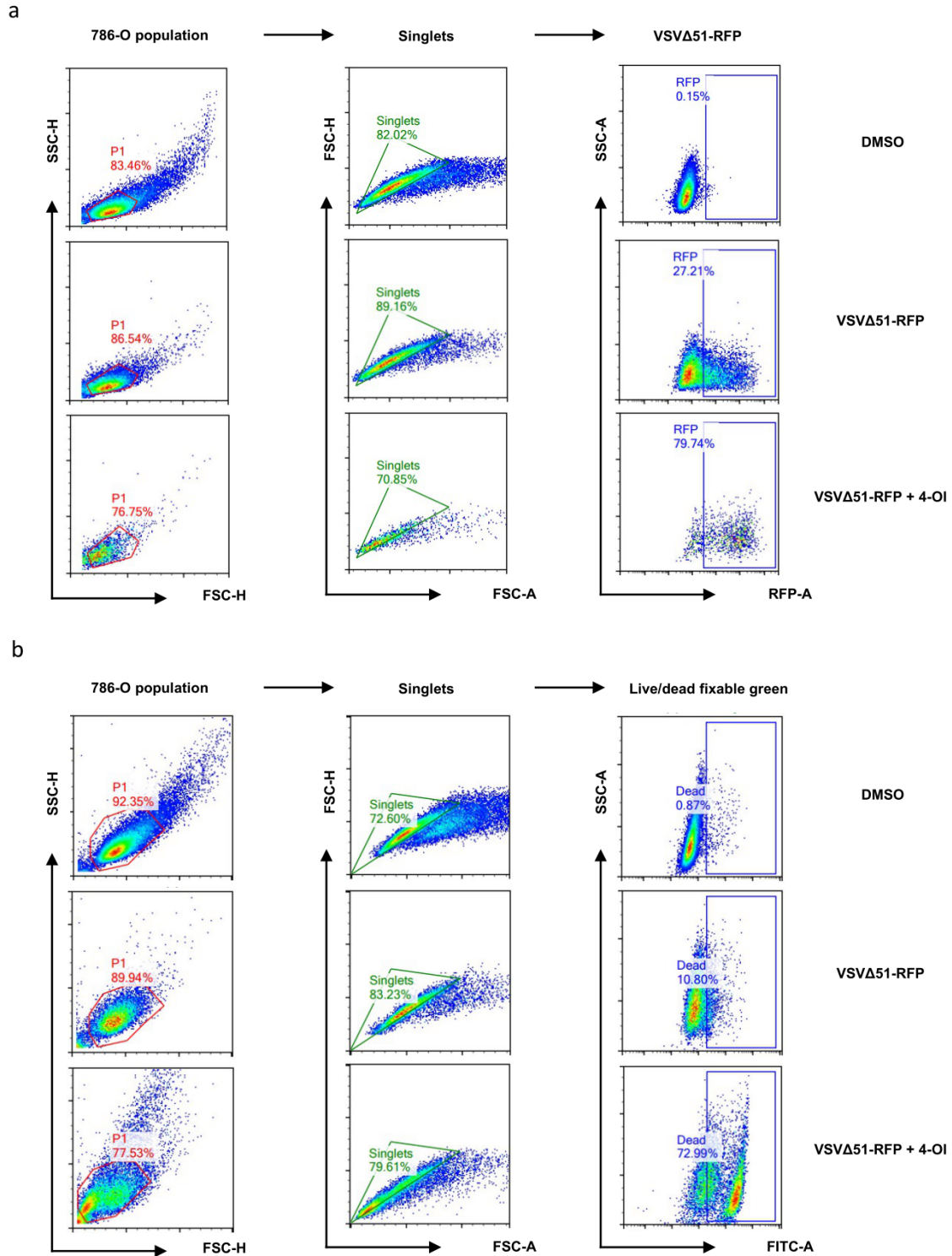


Figure S18. Gating strategies for flow cytometry

a Gating strategy for flow cytometric assessment of viral infection using RFP-expressing virus strain. Fluorescent flow cytometry data scale (RFP-A) is shown in logarithmic flavor ranging from 10^1 - 10^7

b Gating strategy for flow cytometric assessment of cellular viability. Fluorescent flow cytometry data scale (FITC-A) is shown in logarithmic flavor ranging from 10^3 - 10^9

Figure S19. Unprocessed immunoblots.

Fig. 4b

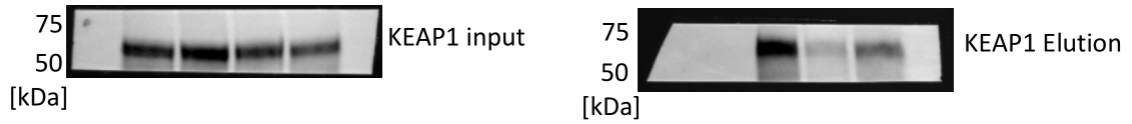


Fig. 4d

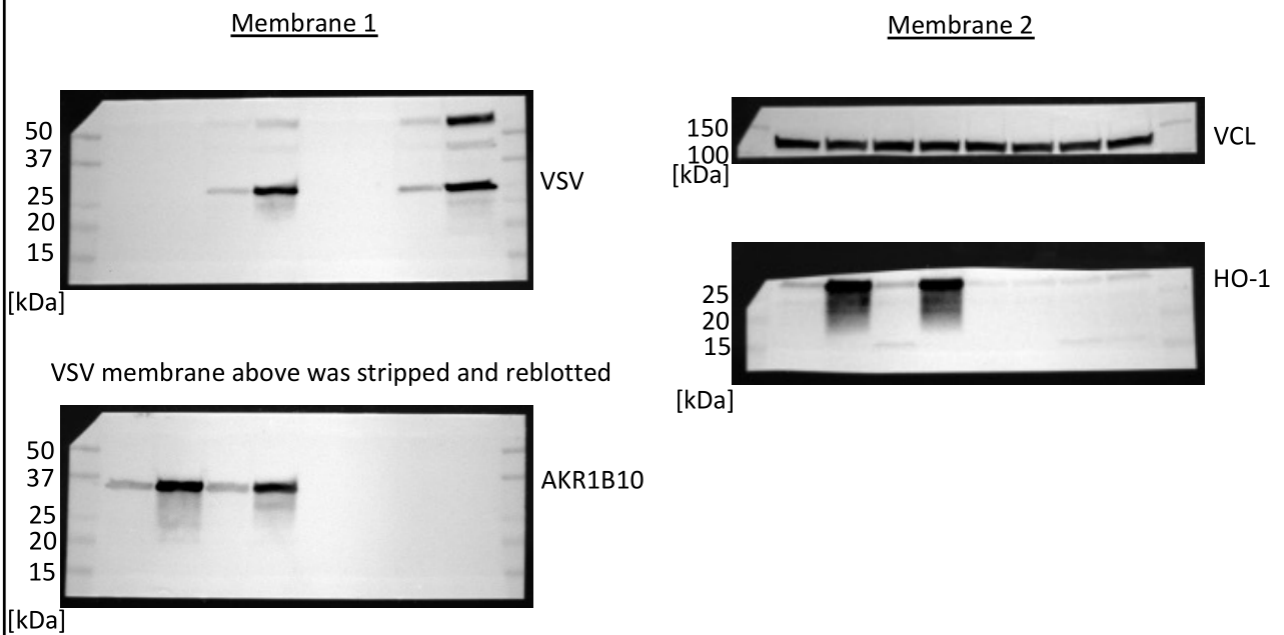


Fig. 4h

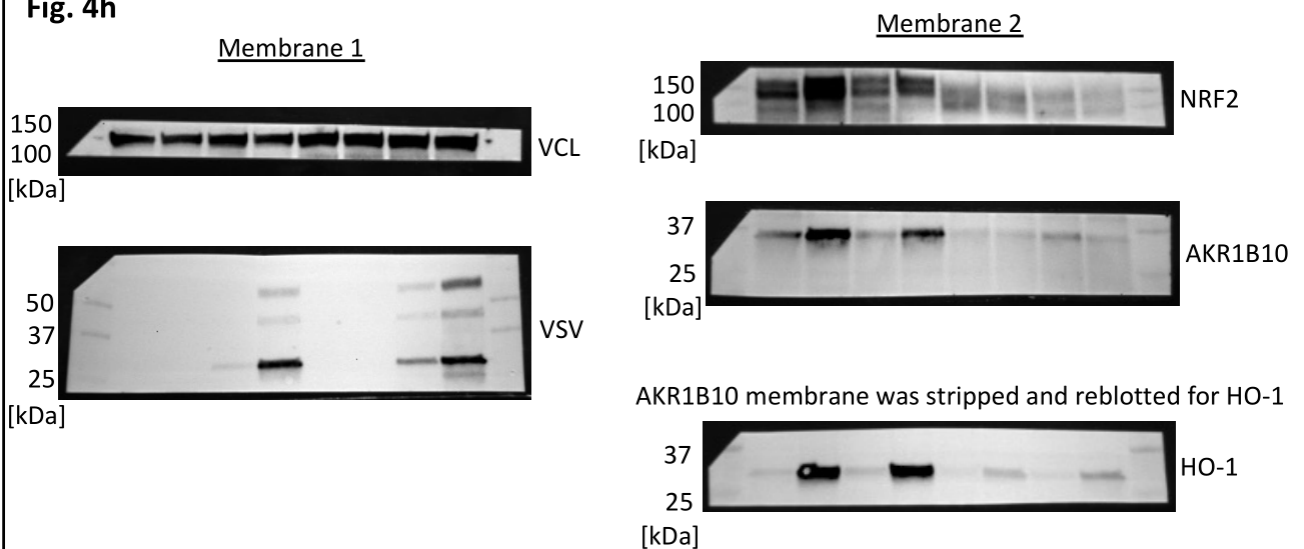


Fig. 4i

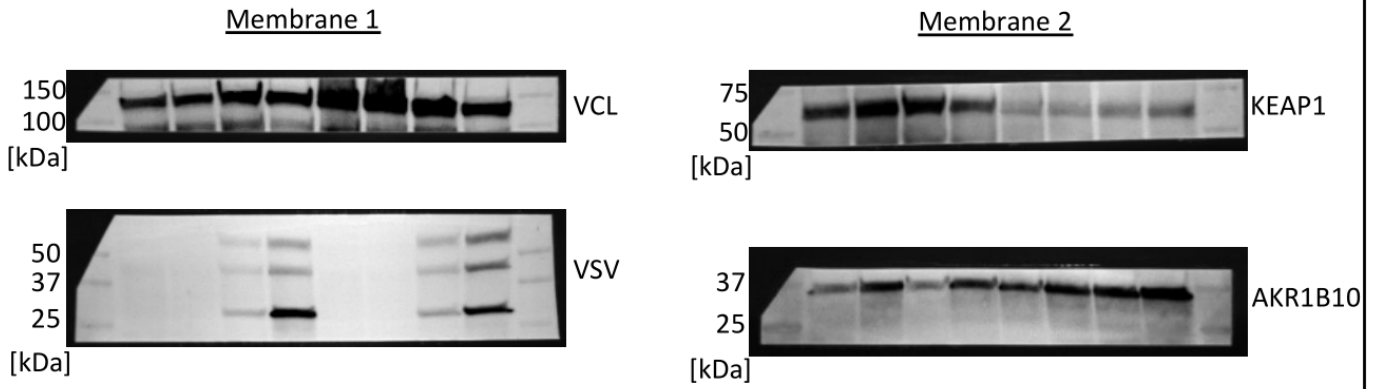
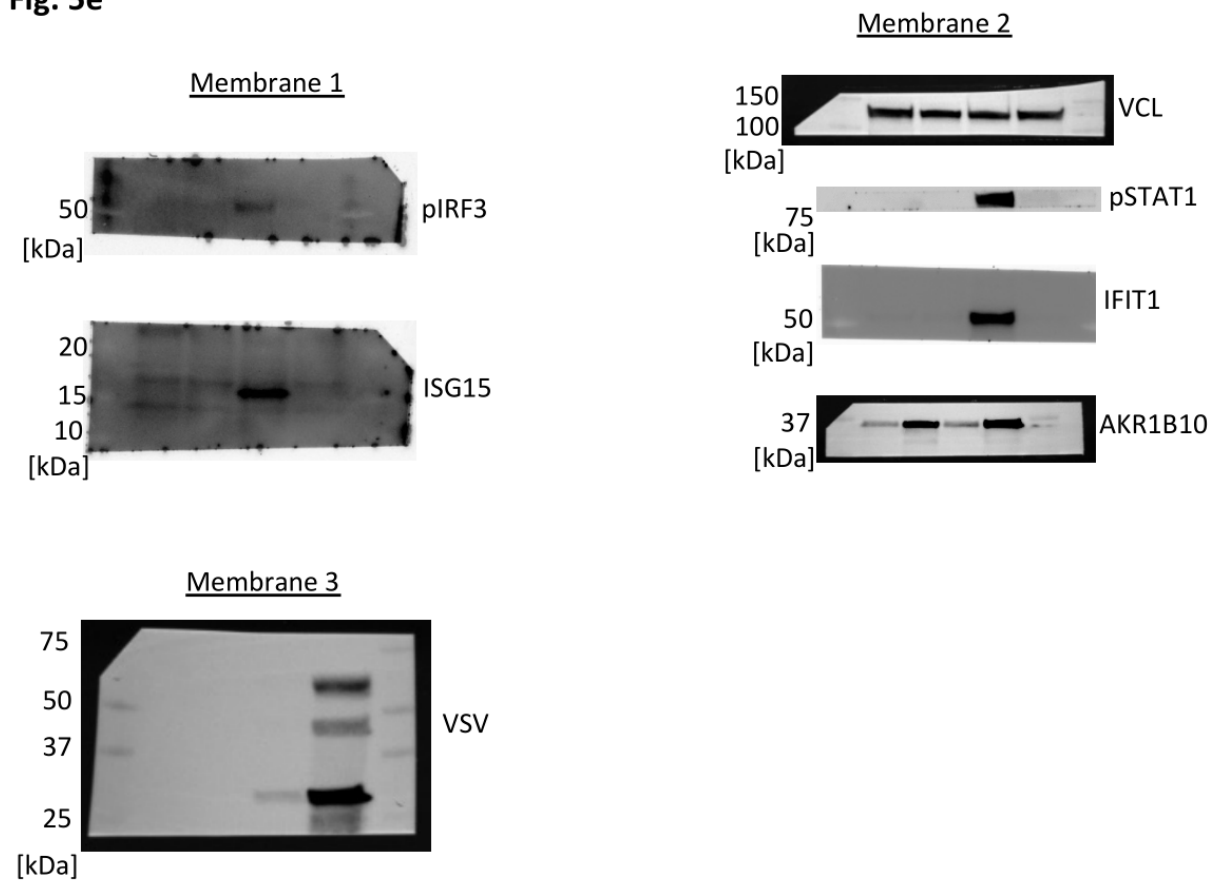


Fig. 5e



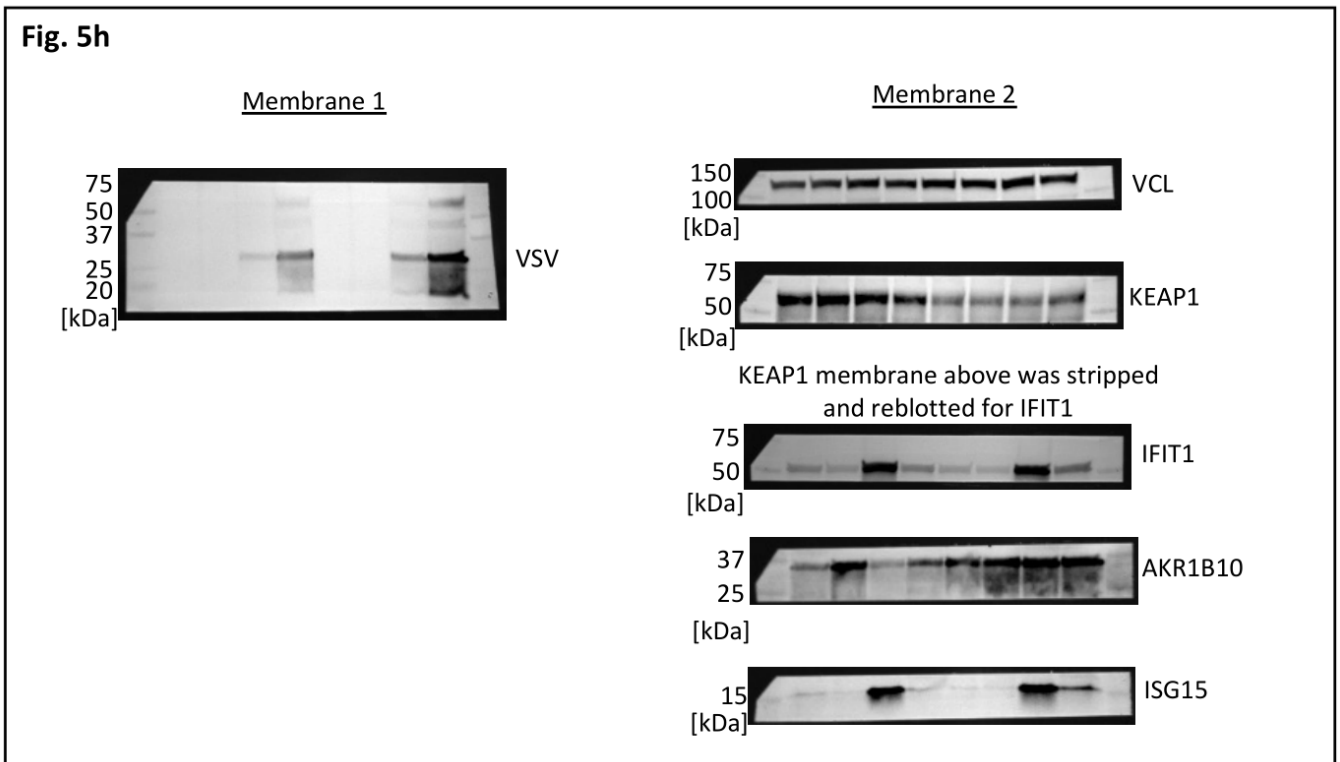
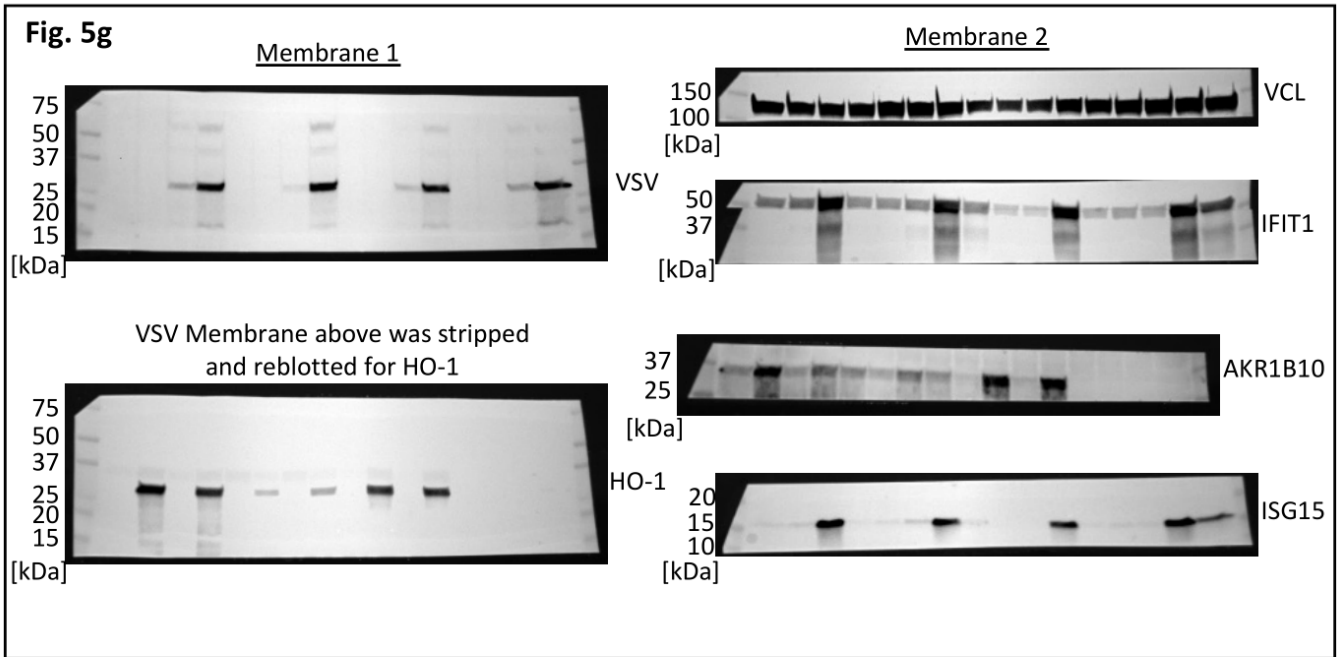


Fig. 5j

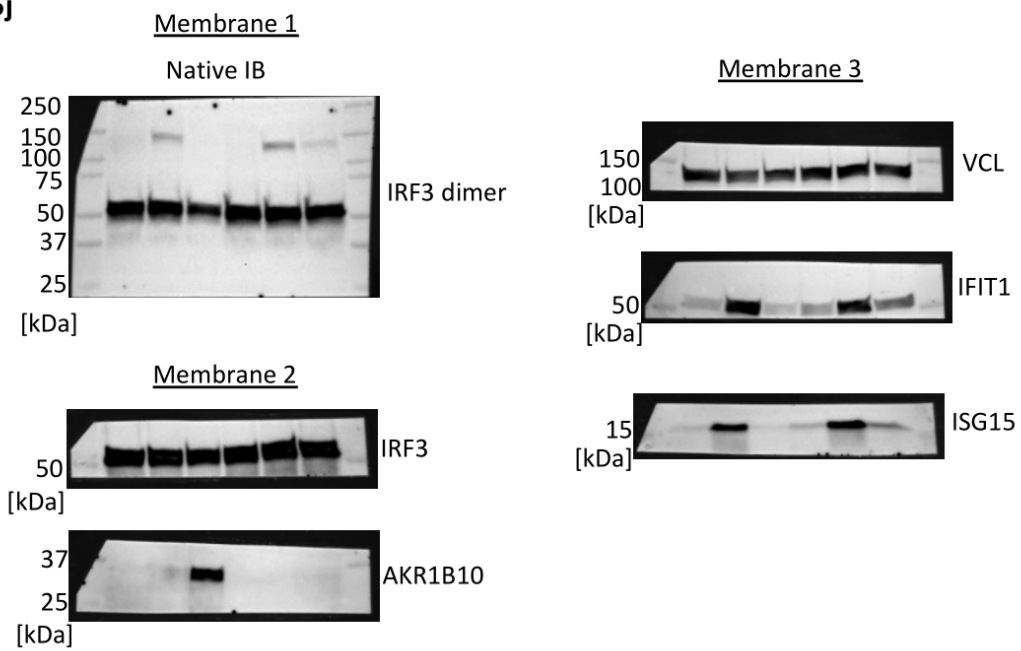


Fig. 7a

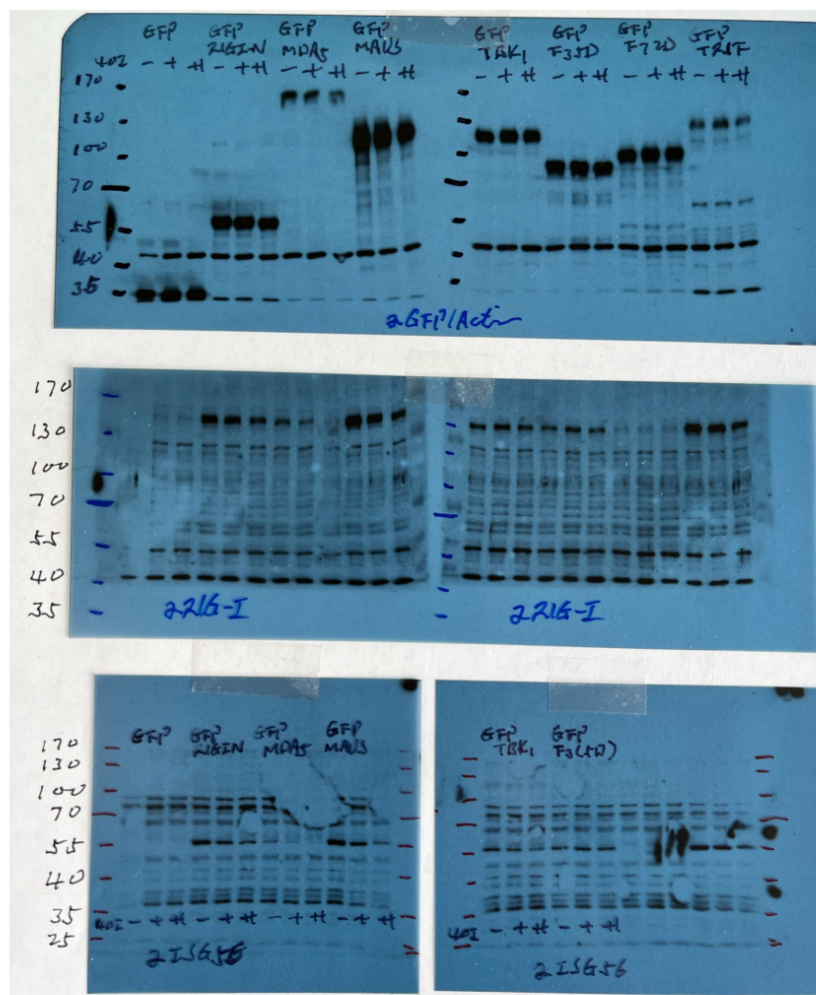


Fig. 7d

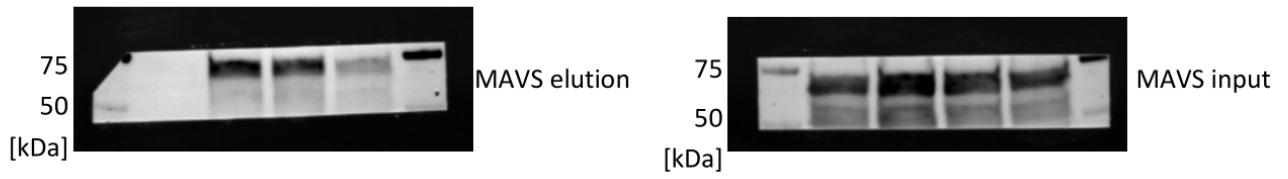


Fig. 7e

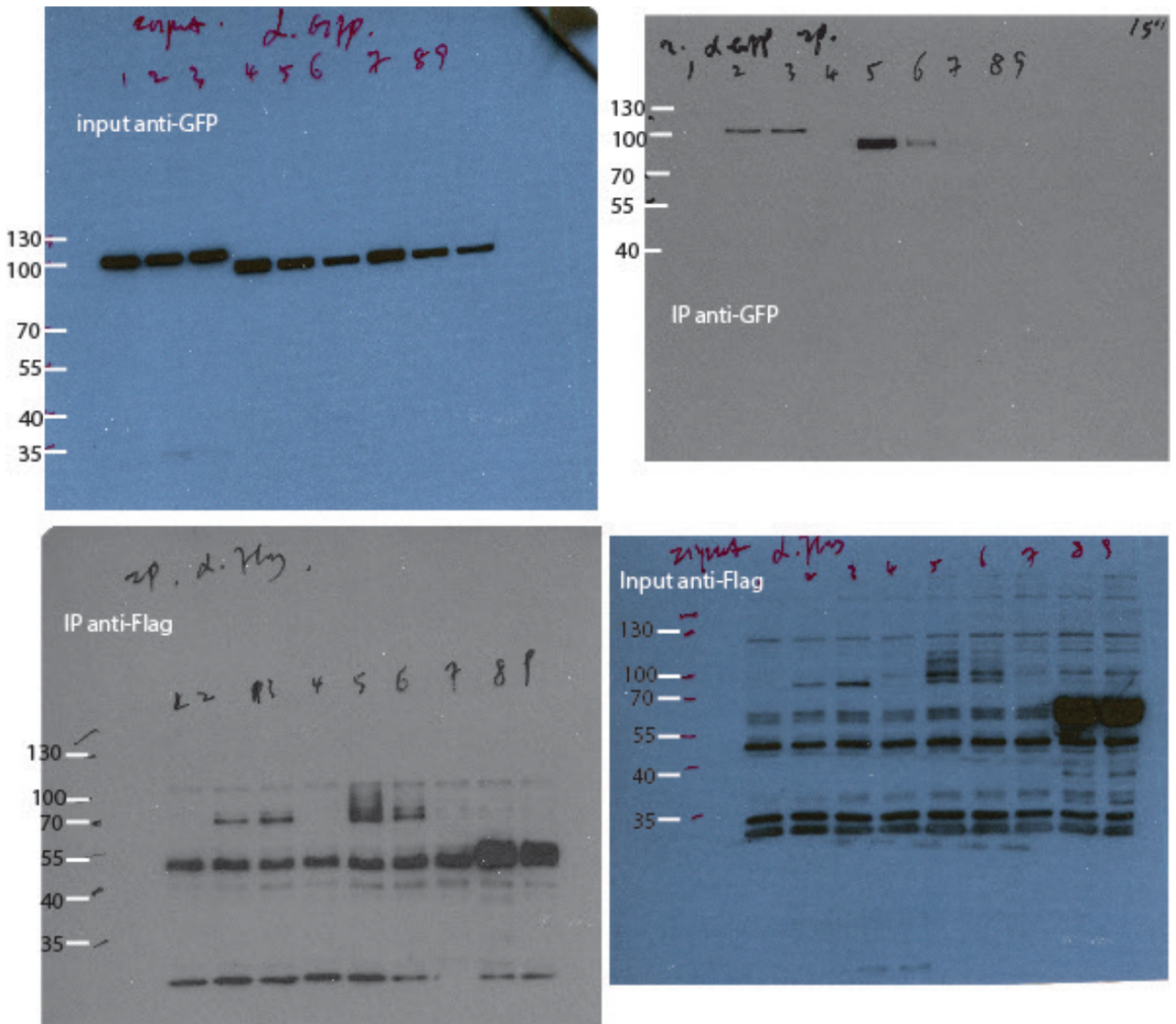


Fig. 7f

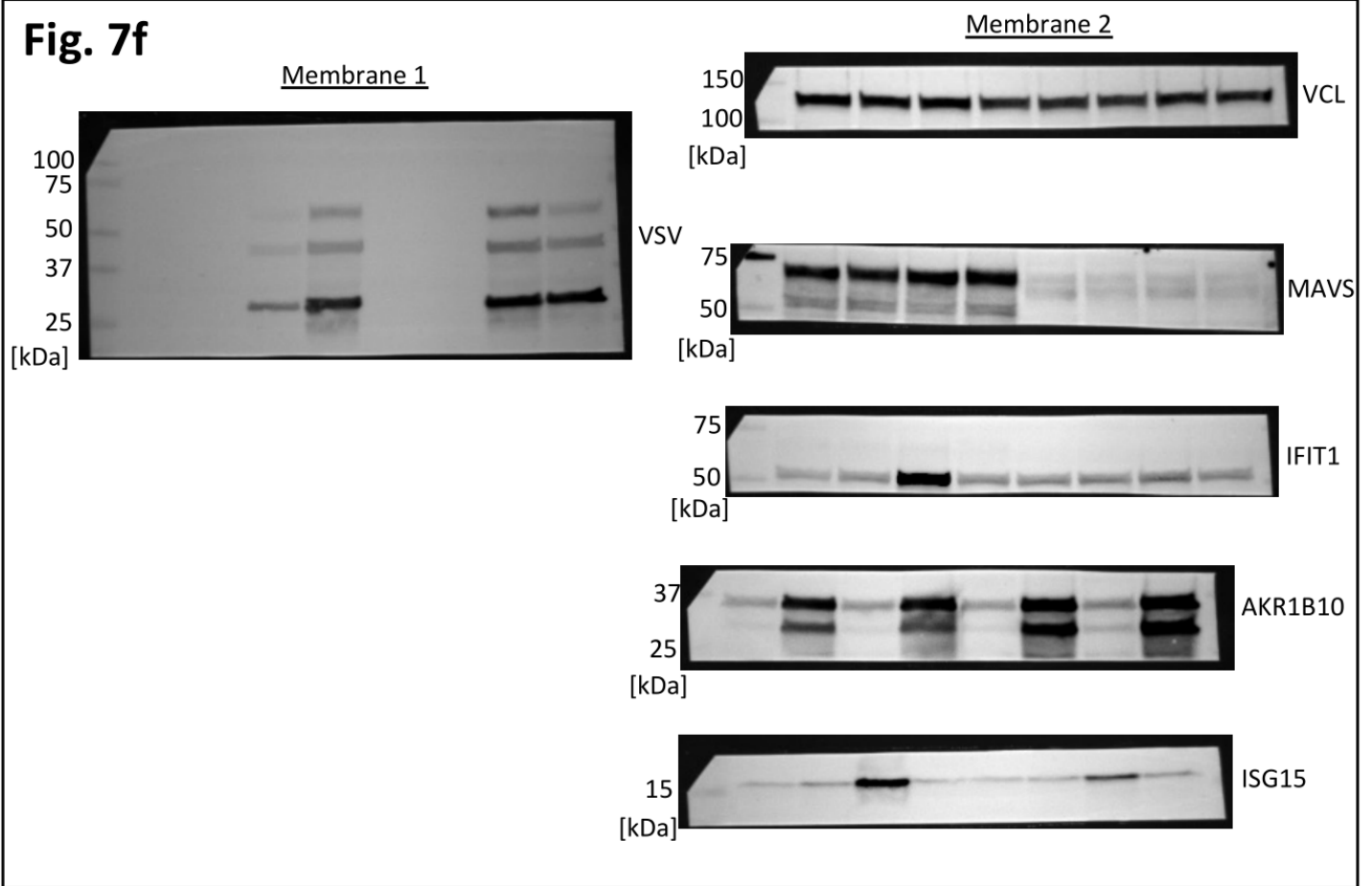


Fig. 7h

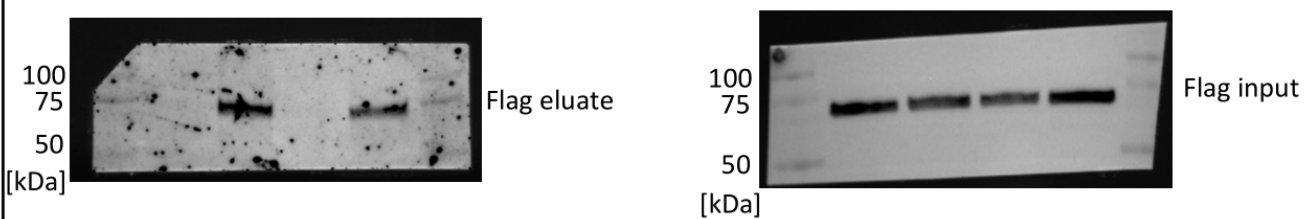


Fig. 7j

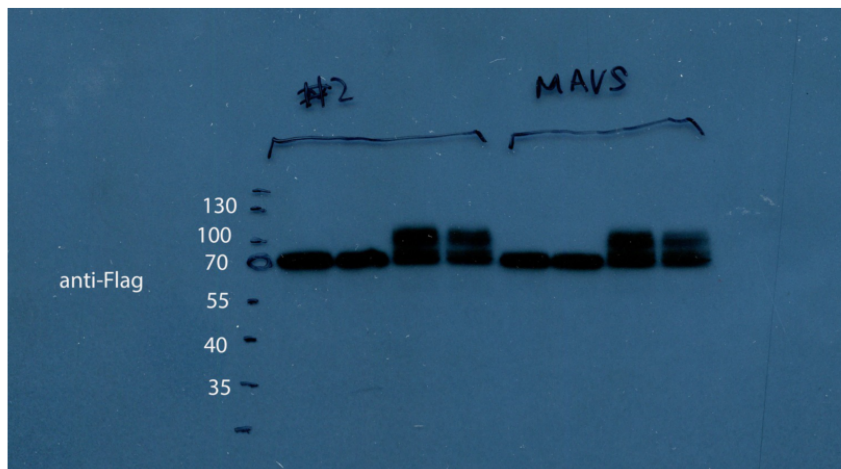
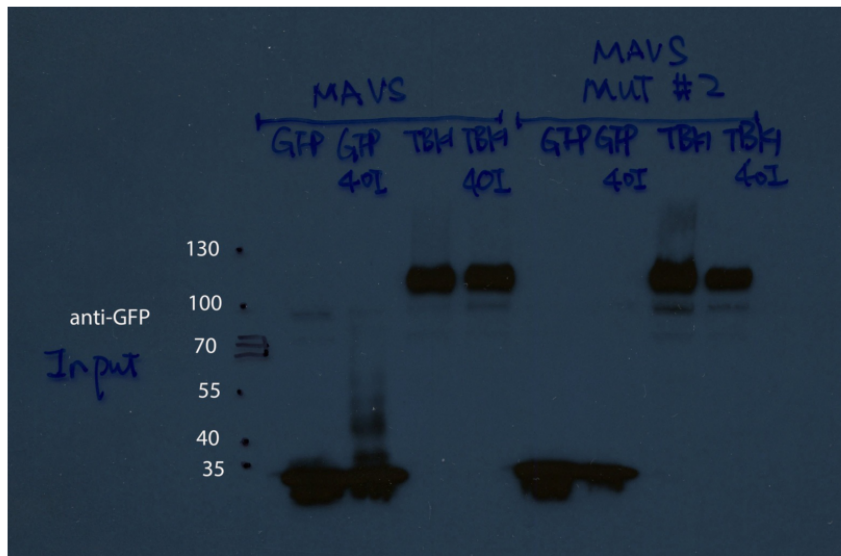
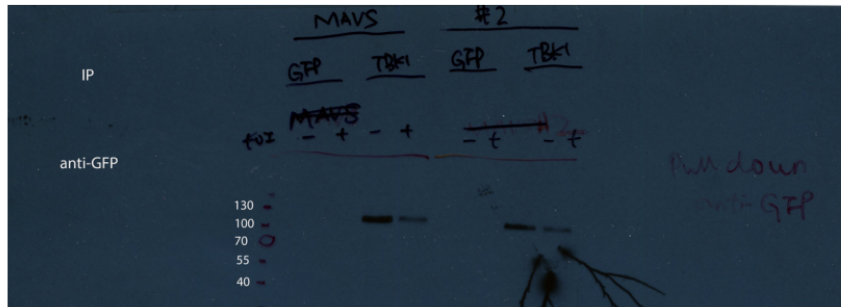
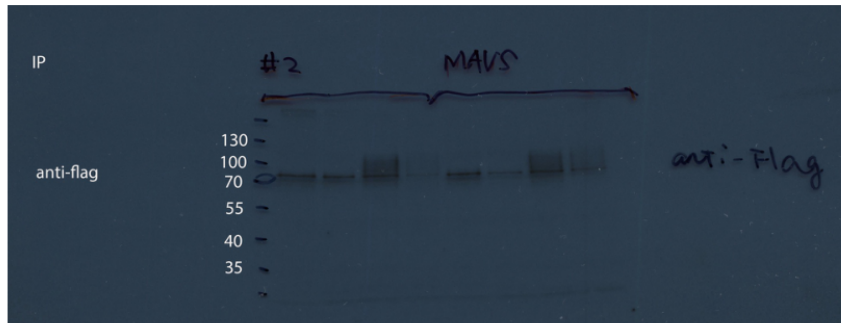


Fig. 8f

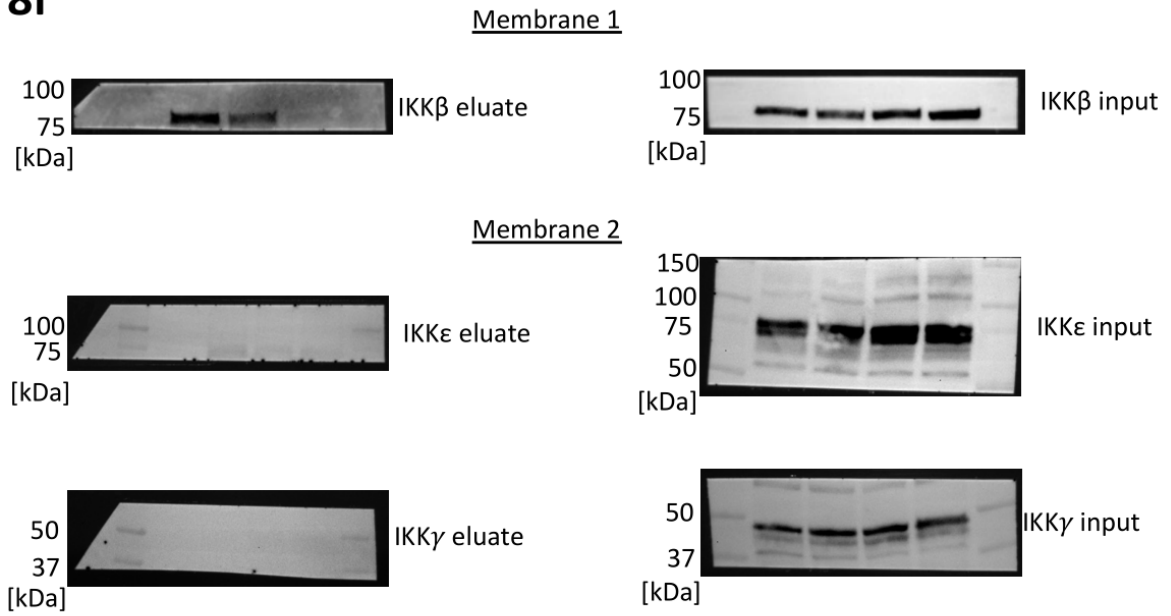


Fig. 8i

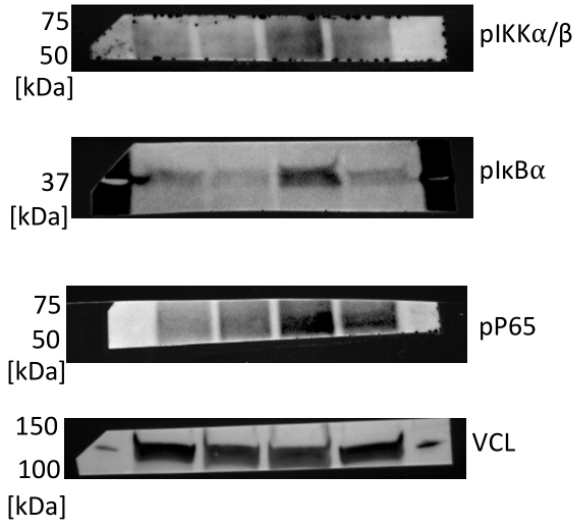


Fig. 8j

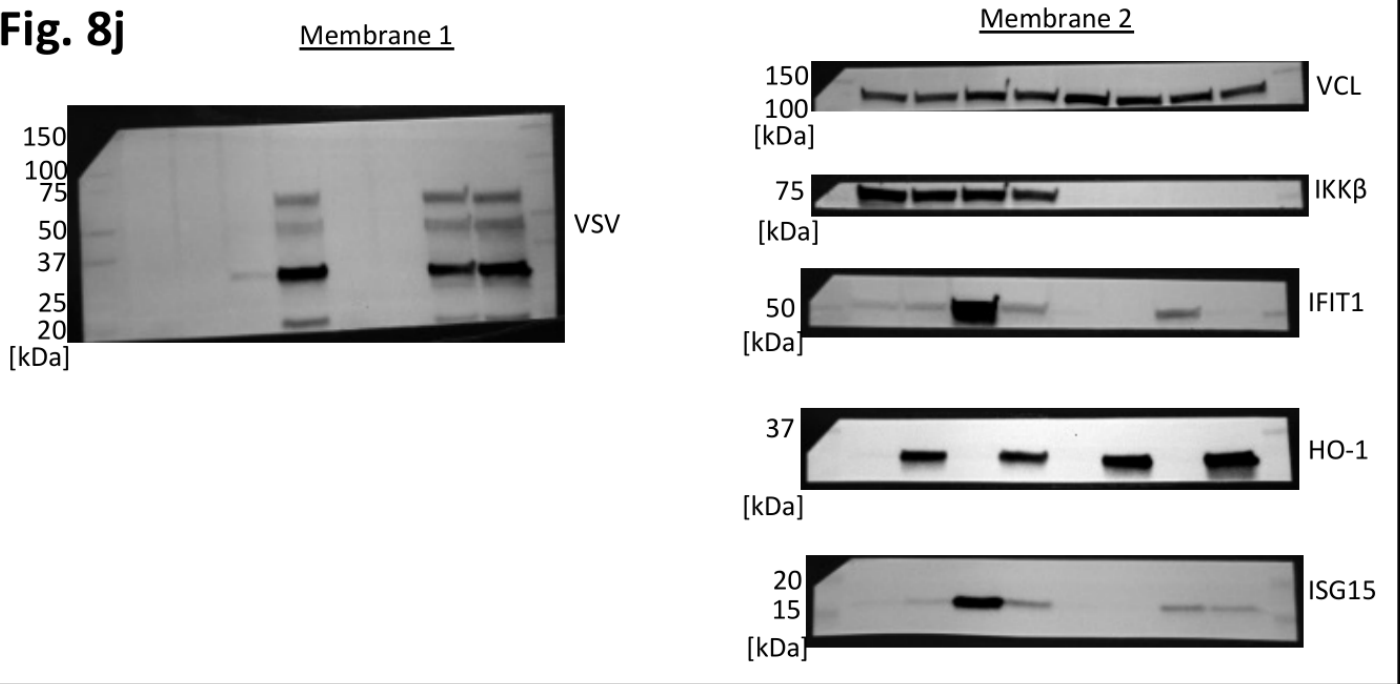


Fig. S8c

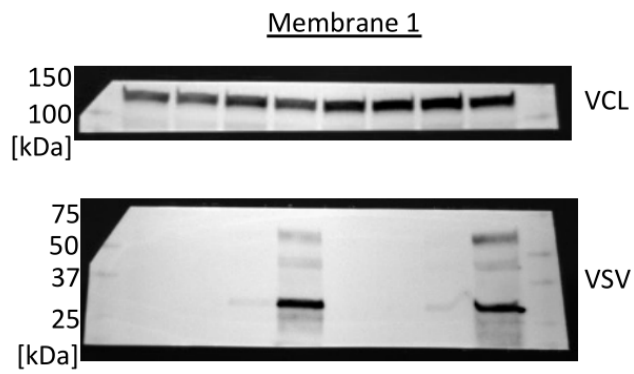


Fig. S9c

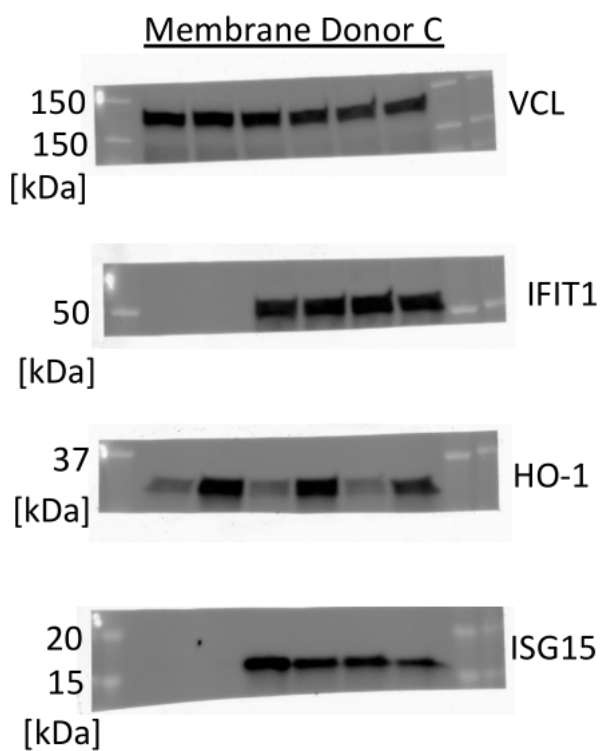
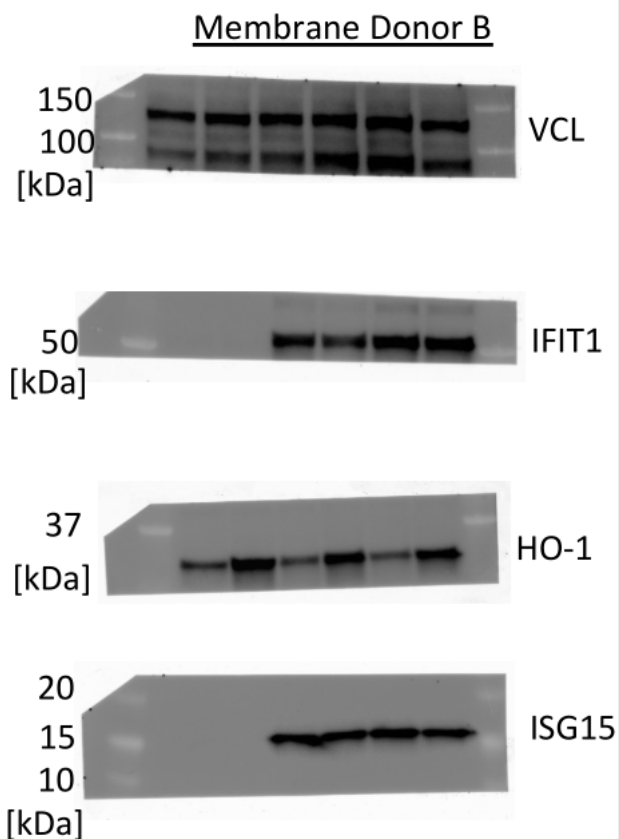
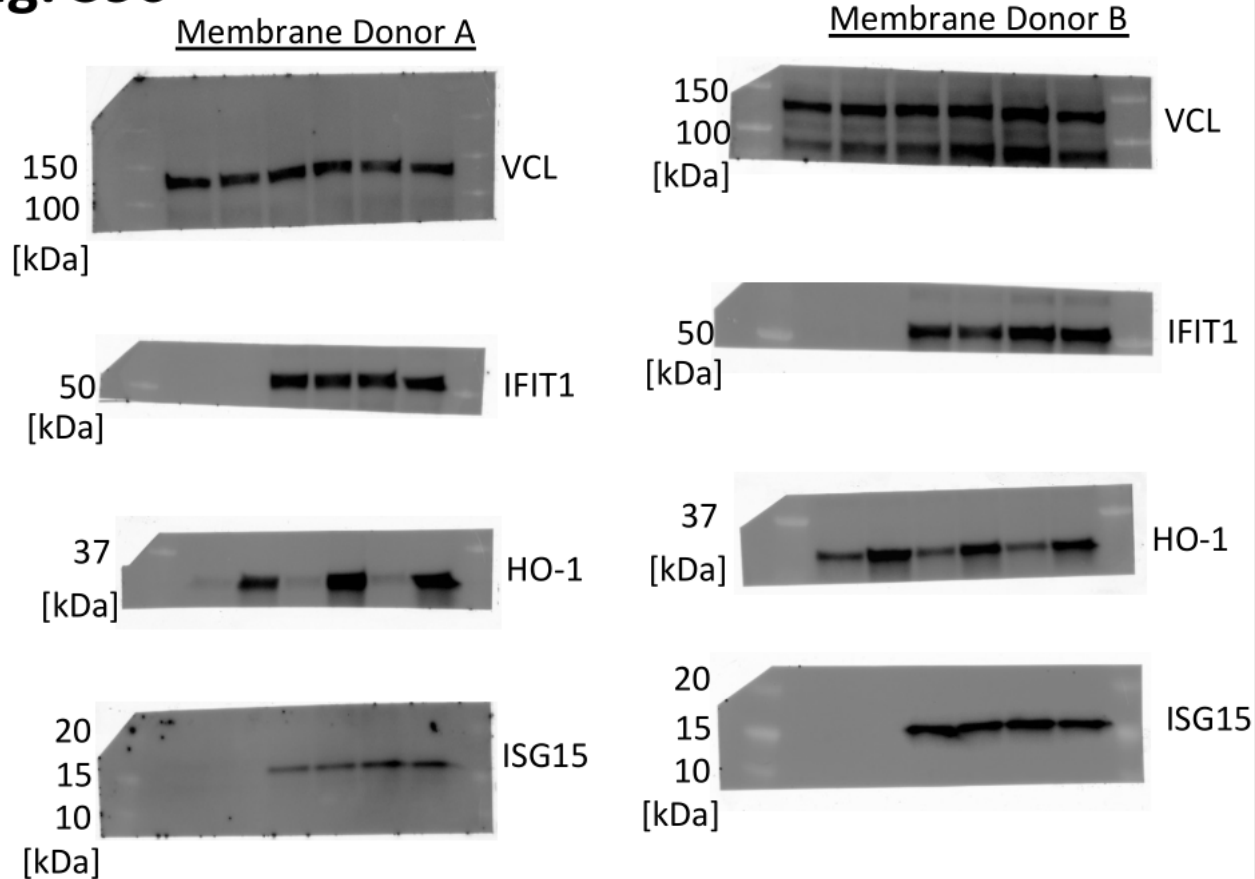


Fig. S9d

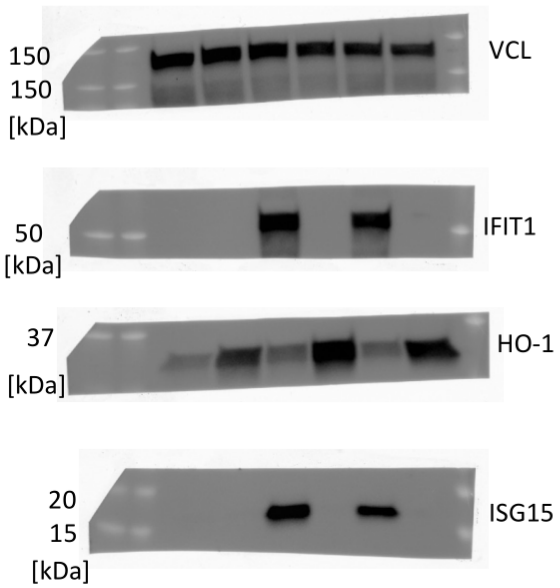
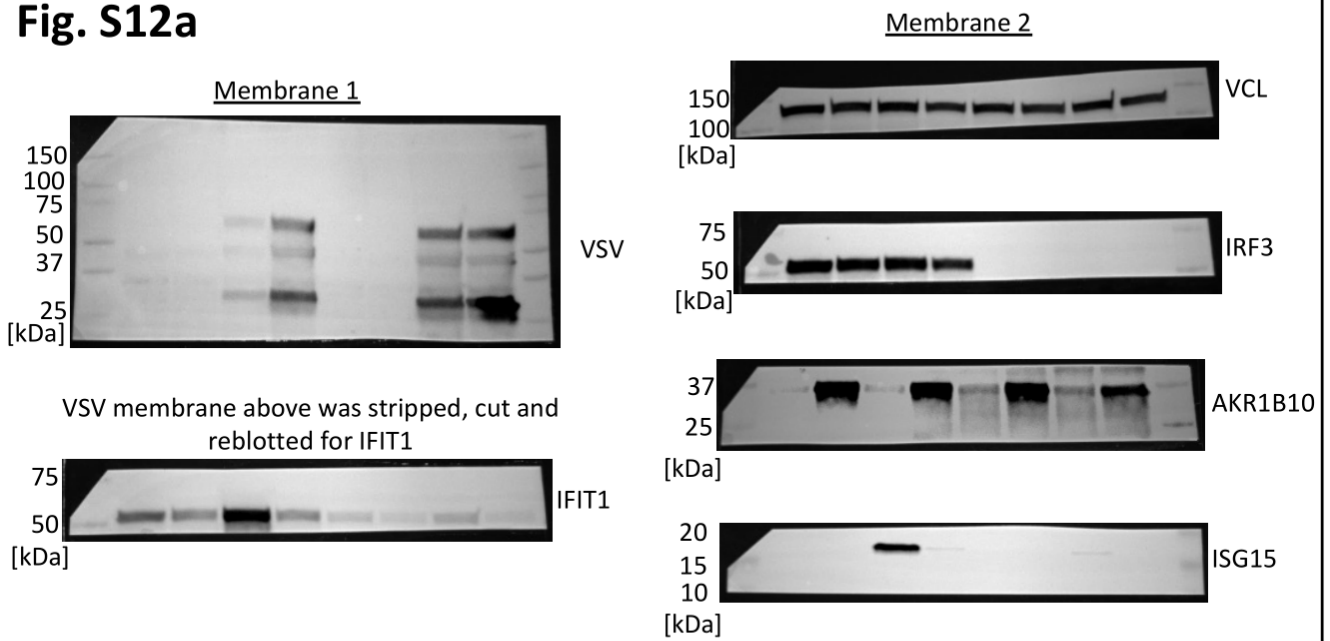


Fig. S12a



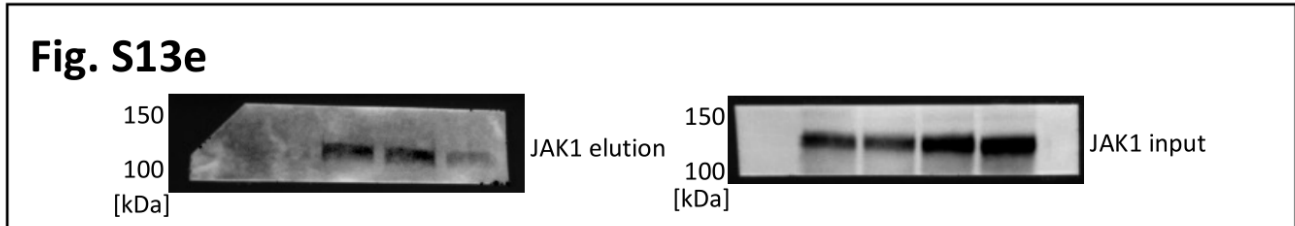
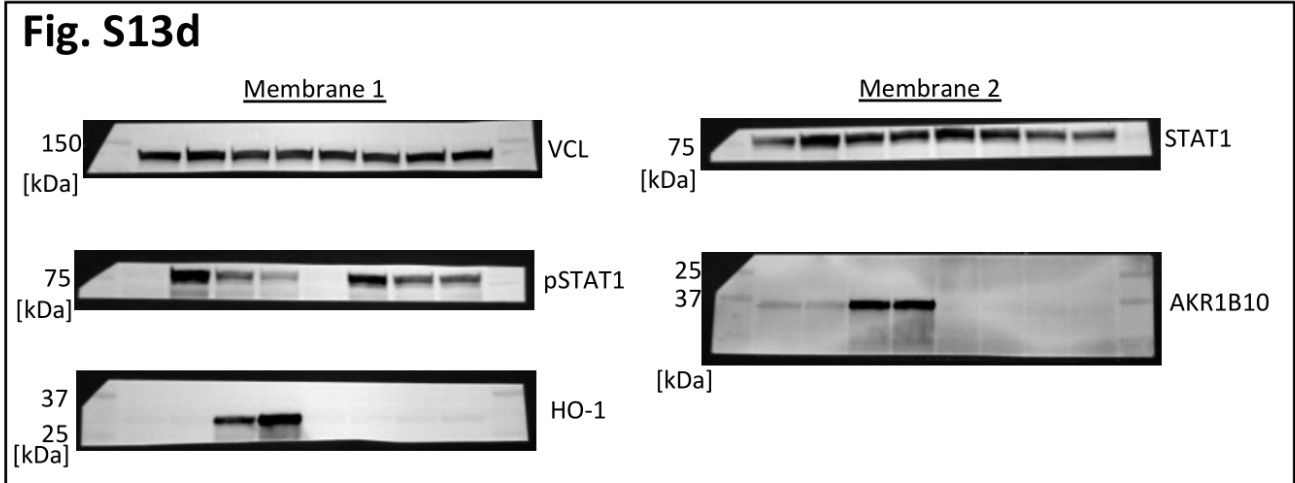
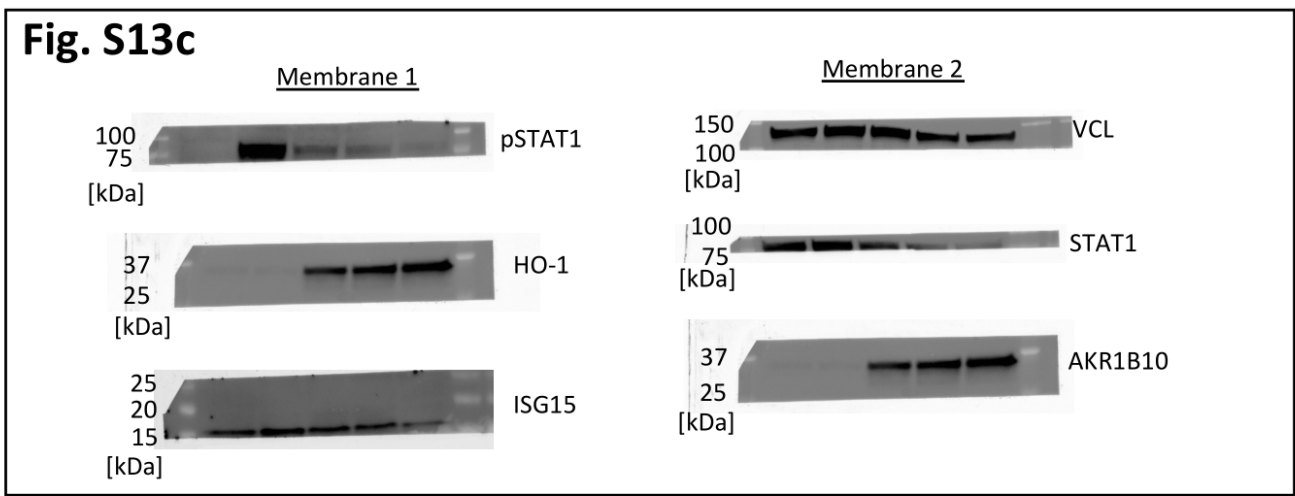
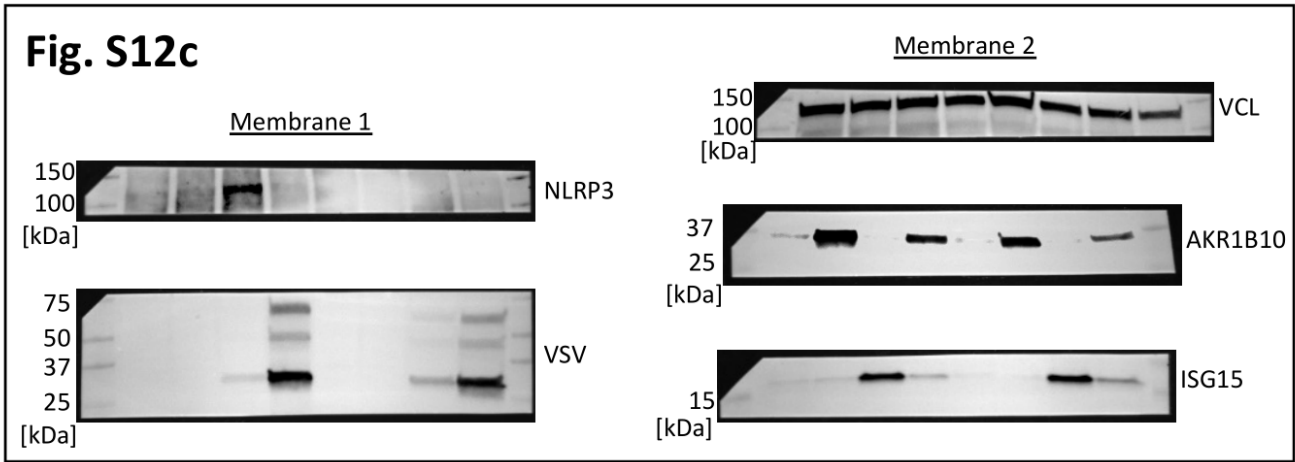


Fig. S13f

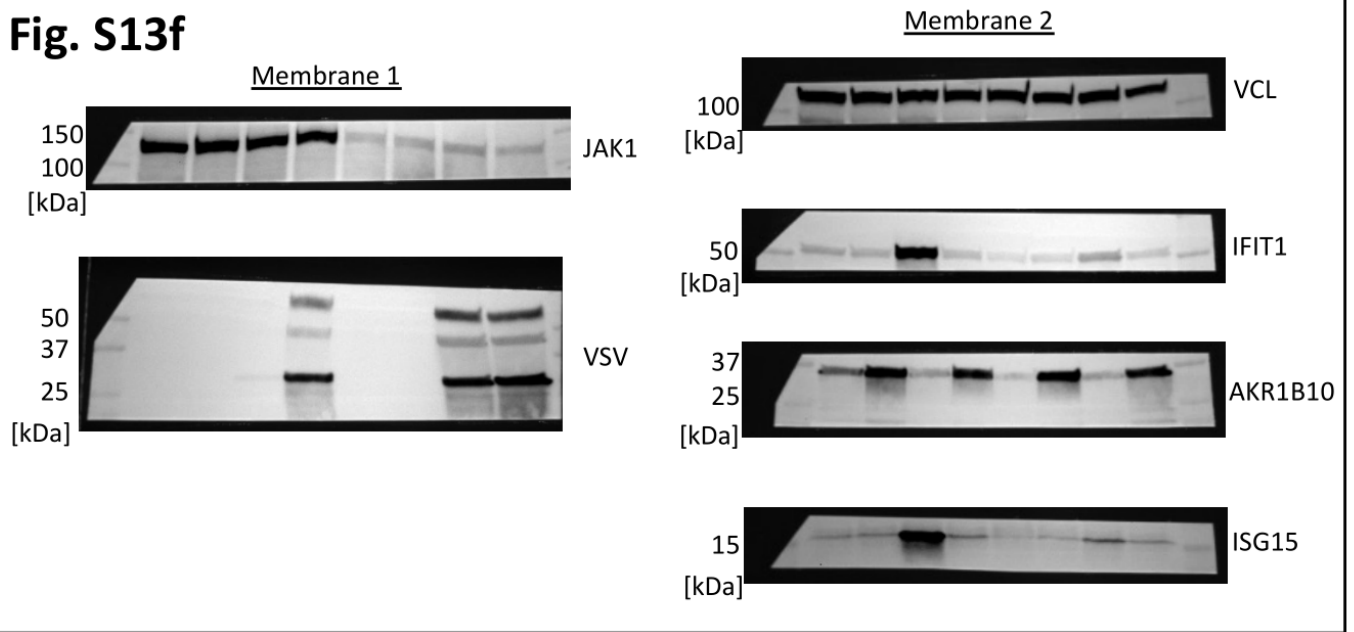


Fig. S15a

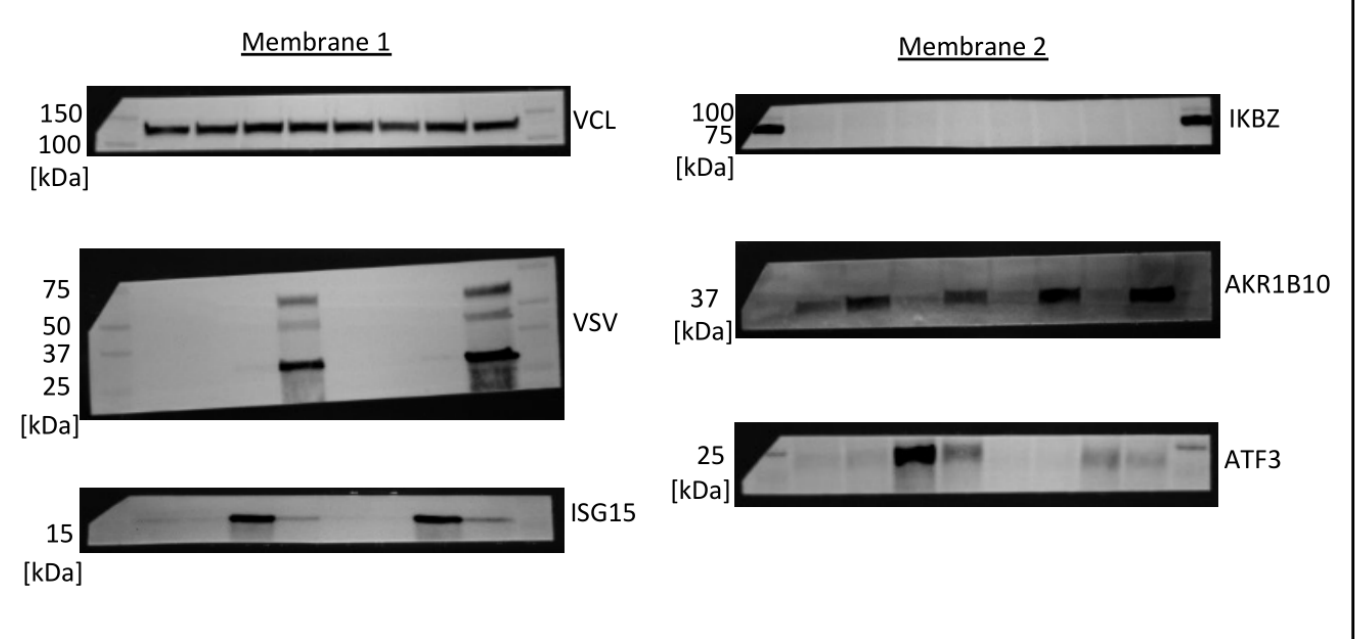


Fig. S15c

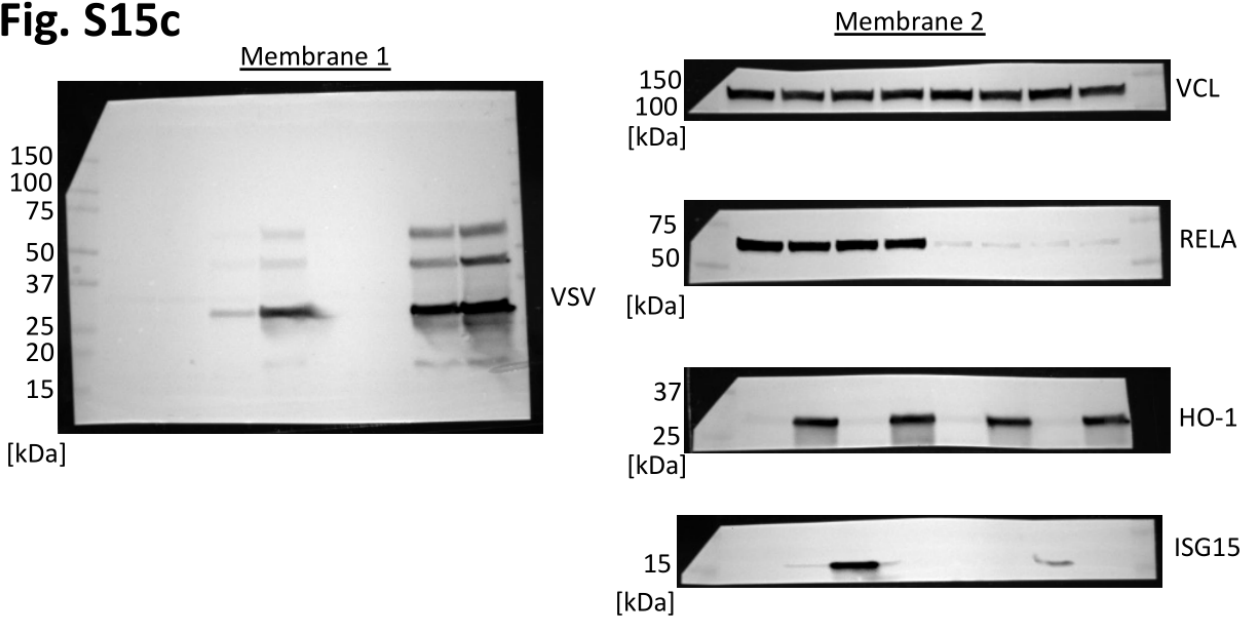
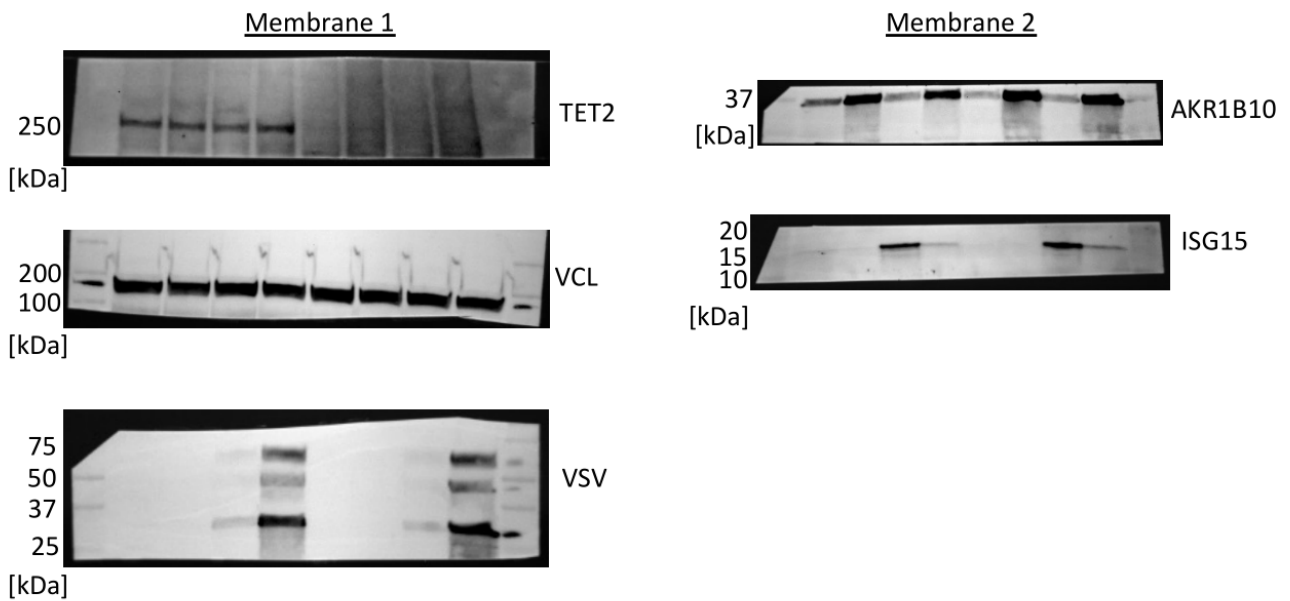


Fig. S15e



Supplementary Tables 1-6

No	Biobank ID (*)	Age	Sex	MMR status (**)	Tumor localization	UICC Classification	Prior Radiation Therapy	Prior Chemotherapy	Normal organoids tested
P1	O17	78	male	MMRp	colon sigmoideum	IIIC	-	-	+
P2	O11	69	male	MMRp	colon sigmoideum	I	-	-	-
P3	O23	59	male	MMRp	rectum	IIIB	+	+	-
P4	O29	79	male	MMRp	colon descendens	IIIB	-	+	-
P5	O06	38	female	MMRp	colon sigmoideum	IIIA	-	-	+
P6	O28	68	male	MMRp	flexura hepatica	IVC	-	-	+
P7	O09	54	male	MMRp	rectum	IIIB	+	+	-
P8	O13	76	male	MMRp	colon descendens	IVB	+	+	-
P9	O24	55	male	MMRp	rectum	IVA	-	+	-
P10	O07	74	female	MMRd	caecum	IVB	-	-	-
P11	O02	78	male	MMRd	colon ascendens	IIA	-	-	-
P12	O14	46	male	MMRp	rectum	I	-	-	-

(*) part of the CRC organoid-stroma biobank (*under review*)

(**) organoids with >1000 somatic alterations detected by whole exome sequencing were defined as mismatch repair deficient (dMMR)

Table S1. Patient characteristics of colorectal organoids used in this study.

ID	Age (Years)	Sex	Tumor localization	Diagnosis
P1	78	Female	Left, occipital	Metastasis, malignant melanoma
P2	75	Male	Left, frontal	Newly diagnosed GBM, IDH-wt (WHO IV)
P3	60	Male	Right, parietal	Recurrent GBM, IDH-wt (WHO IV), radiochemotherapy

Table S2. Clinical data from all brain tumor patients.

Binding site	IKK β Binding energy score (S) (kcal/mol)
Cys12	-6.8 to -7.6
Cys179	-7.0 to -8.1
Cys412	-8.2 to -10.0
Cys464	-7.7 to -9.0
Cys524	-6.5 to -7.1
Cys716	-5.1 to -5.7

Table S3. Binding energies of 4-OI to different cysteine-containing sites in IKK β .

Fluorochrome	Target	Clone	Category number	Vendor	Dilution	Panel
AF700	CD8	53-6.7	56-0081-82	Thermofisher	1:100	T-cell
AF700	CD45.2	104	109822	Biologend	1:400	Myeloid
APC	NKG2a	16A11	142807	Biologend	1:100	T-cell
APC	XCR1	ZET	148206	Biologend	1:200	Myeloid
APC-Cy7	PD1	29F.1A12	135224	Biologend	1:50	T-cell
APC-Cy7	CD11c	N418	117324	Biologend	1:100	Myeloid
BV421	CD62L	MEL-14	104436	Biologend	1:100	T-cell
BV421	MHC-II	M5/114	562564	BD	1:400	Myeloid
BV510	Zombie Aqua		423101	Biologend	1:800	All
BV605	CD69	H1.2F3	104530	Biologend	1:100	T-cell
BV605	Ly6C	HK1.4	128036	Biologend	1:500	Myeloid
BV650	NK1.1	PK136	564143	BD	1:100	T-cell
BV650	Siglec-H	440c	747672	BD	1:300	Myeloid
BV711	CD4	RM4-5	100549	Biologend	1:200	T-cell
BV711	CD103	2E7	121435	Biologend	1:200	Myeloid
BV786	CD44	IM7	103059	Biologend	1:100	T-cell
BV786	Ly6G	1A8	127645	Biologend	1:400	Myeloid
FITC	CD45.2	104	109806	Biologend	1:200	T-cell
FITC	CD11b	ICRF44	562793	BD	1:500	Myeloid
PE	Foxp3	FJK-16s	12-5773-80	Thermofisher	1:200	T-cell
PE	CD86	GL-1	105007	Biologend	1:400	Myeloid
PECF594	CD3	145-2C11	562286	BD	1:200	All
PE-Cy7	KLRG-1	2F1	25-5893-82	Invitrogen	1:200	T-cell
PE-Cy7	F4/80	BM8	123112	Biologend	1:100	Myeloid
	CD16/CD32	2.4G2	553142	BD	1:250	All

Table S4. Listing of antibodies used in the *in vivo* immunophenotyping experiment.

Target	F/R	Sequence
VSV	Forward	CCTGATGACATTGAGTATACATCTCTT
VSV	Reverse	GGATCCTACTGCATAAGCGTACA
ISG15	Forward	GGAACGAAAGGGGCCACAGCA
ISG15	Reverse	CCTCCATGGGCCTTCCCTCGA
NFKB	Forward	CACCTAGCTGCCAAAGAAGG
NFKB	Reverse	GCAGGCTATTGCTCATACA
CXCL9	Forward	TGGAGTTCGAGGAACCCTAGT
CXCL9	Reverse	AGGCAGGTTTGTCTCCGTT
Mzt2	Forward	TCGGTGCCCATATCTCTGTC
Mzt2	Reverse	CTGCTTCGGGAGTTGCTTTT
Ptp4a	Forward	AGCCCTGTGGAGATCTCTT
Ptp4a	Reverse	AGCATCACAACTCGAACCA
MX1	Forward	CTGGAAGCACTGTCTGGAGT
MX1	Reverse	GGCCTCTTCCACCTCTGAAG
HMOX1	Forward	GGTCAGGTGTCCAGAGAAGG
HMOX1	Reverse	ATGATTTCTGCCAGTGAGG
IL6	Forward	AACGATGATGCACTTGCAGA
IL6	Reverse	CTCTGAAGGACTCTGGCTTTG
IFIT1	Forward	CTGGACAAGGTGGAGAAGGT
IFIT1	Reverse	AGGGTTTTCTGGCTCCACTT
IL1b	Forward	GACCTTCCAGGATGAGGACA
IL1b	Reverse	AGCTCATATGGGTCCGACAG
TNF	Forward	GAAGTGGCAGAAGAGGCACT
TNF	Reverse	AGGGTCTGGGCCATAGAACT
IFNbeta	Forward	AGAAAGGACGAACATTCGGAAA
IFNbeta	Reverse	CCGTCATCTCCATAGGGATCTT
Viperin	Forward	TTGGGCAAGCTTGTGAGATTC
Viperin	Reverse	TGAACCATCTCTCTGGATAAGG

Table S5. Listing of the primers used for the *in vivo* intratumoral qPCR experiments.

Name	Sequence
hsMx1-F	GTTTCCGAAGTGGACATCGCA
hsMx1-R	CTGCACAGTTGTCTCAGC
hslSG15-F	CGCAGATCACCCAGAAGATCG
hslSG15-R	TTCGTGCAATTTGTCCACCA
hslFNB1-F	ATGACCAACAAGTGTCTCCTCC
hslFNB1-R	GGAATCCAAGCAAGTTGTAGCTC
hslFIT1-F	TTGATGACGATGAAATGCCTGA
hslFIT1-R	CAGGTCACCAGACTCCTCAC
hsTNF-F	CCTCTCTAATCAGCCCTCTG
hsTNF-R	GAGGACCTGGGAGTAGATGAG
hslL6-F	ACTCACCTCTCAGAACGAATTG
hslL6-R	CCATCTTTGGAAGGTTCCAGGTTG
hslL1b-F	ATGATGGCTTATTACAGTGGCAA
hslL1b-R	GTCGGAGATTCGTAGCTGGA
hsHPRT1-F	CCTGGCGTCGTGATTAGTGAT
hsHPRT1-R	AGACGTTCAAGTCTGTCCATAA

Table S6. Listing of the primers used for qPCR on measles, reovirus and vaccinia virus-infected cells.

Supplementary Methods

Copies of NMR spectra

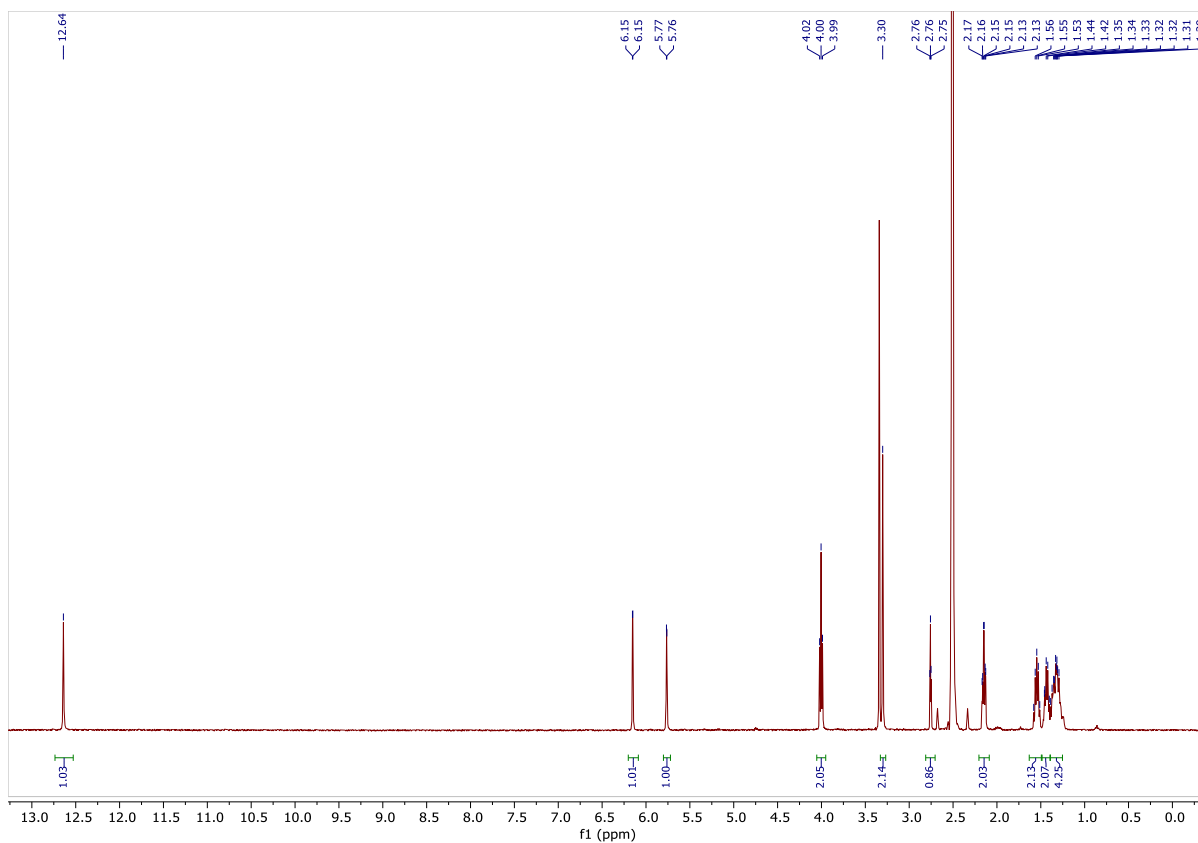


Figure: ^1H NMR spectrum (400 MHz, $\text{DMSO-}d_6$) of 4-OI-alk

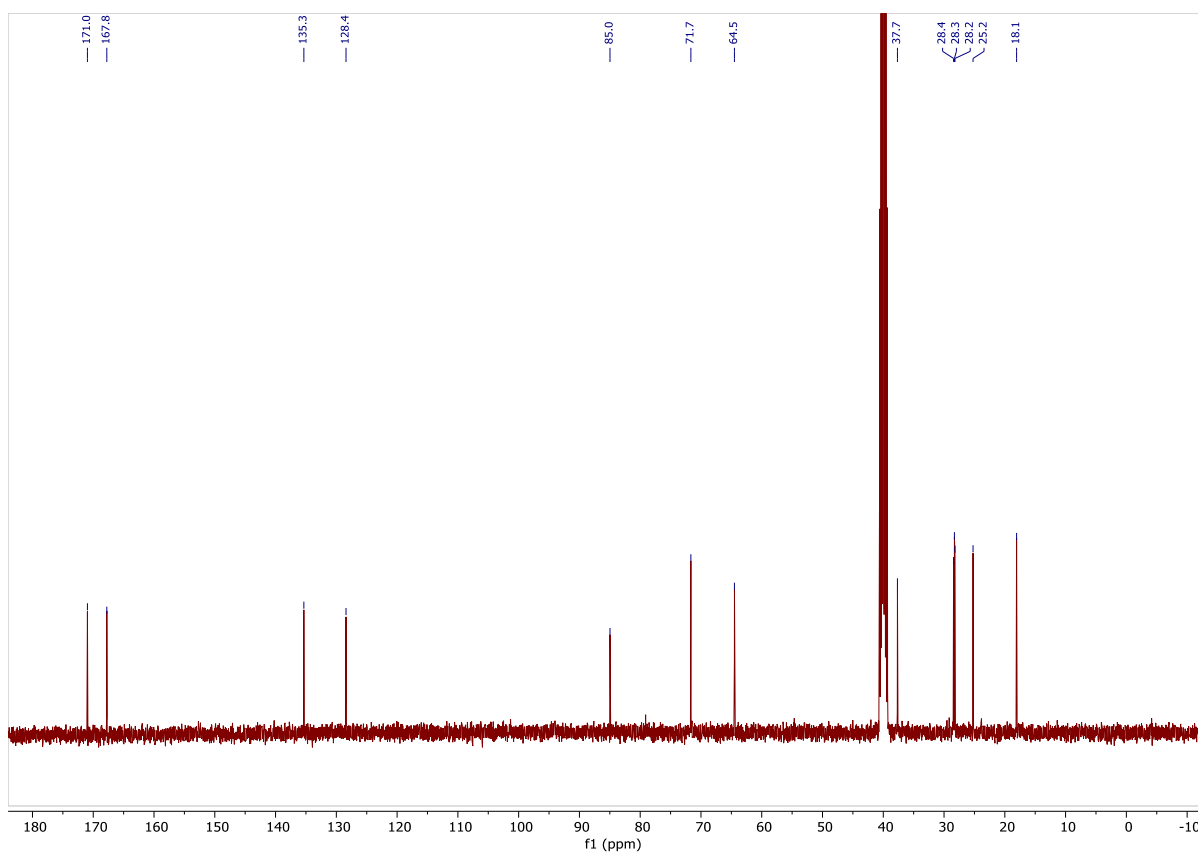


Figure: ^{13}C NMR spectrum (101 MHz, $\text{DMSO-}d_6$) of 4-OI-alk

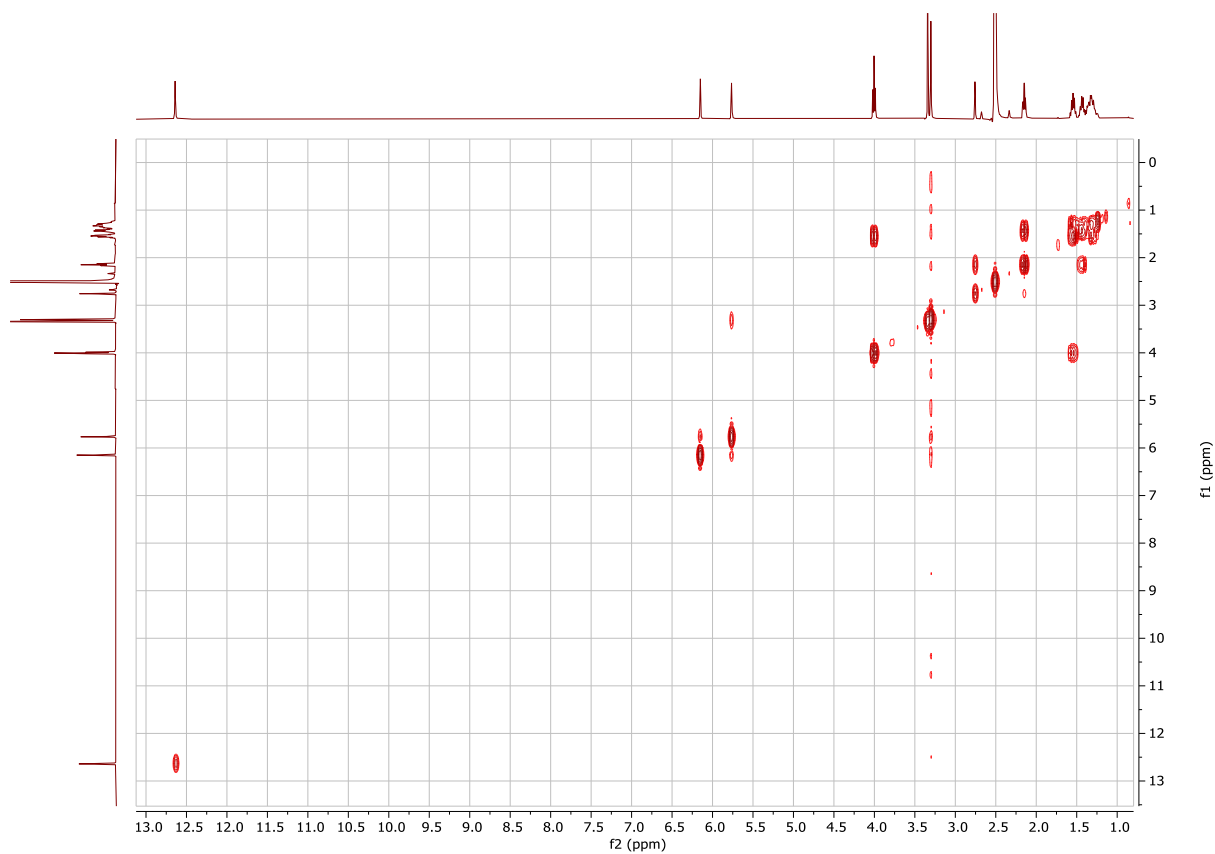


Figure: COSY spectrum (400 MHz, DMSO- d_6) of **4-OI-alk**

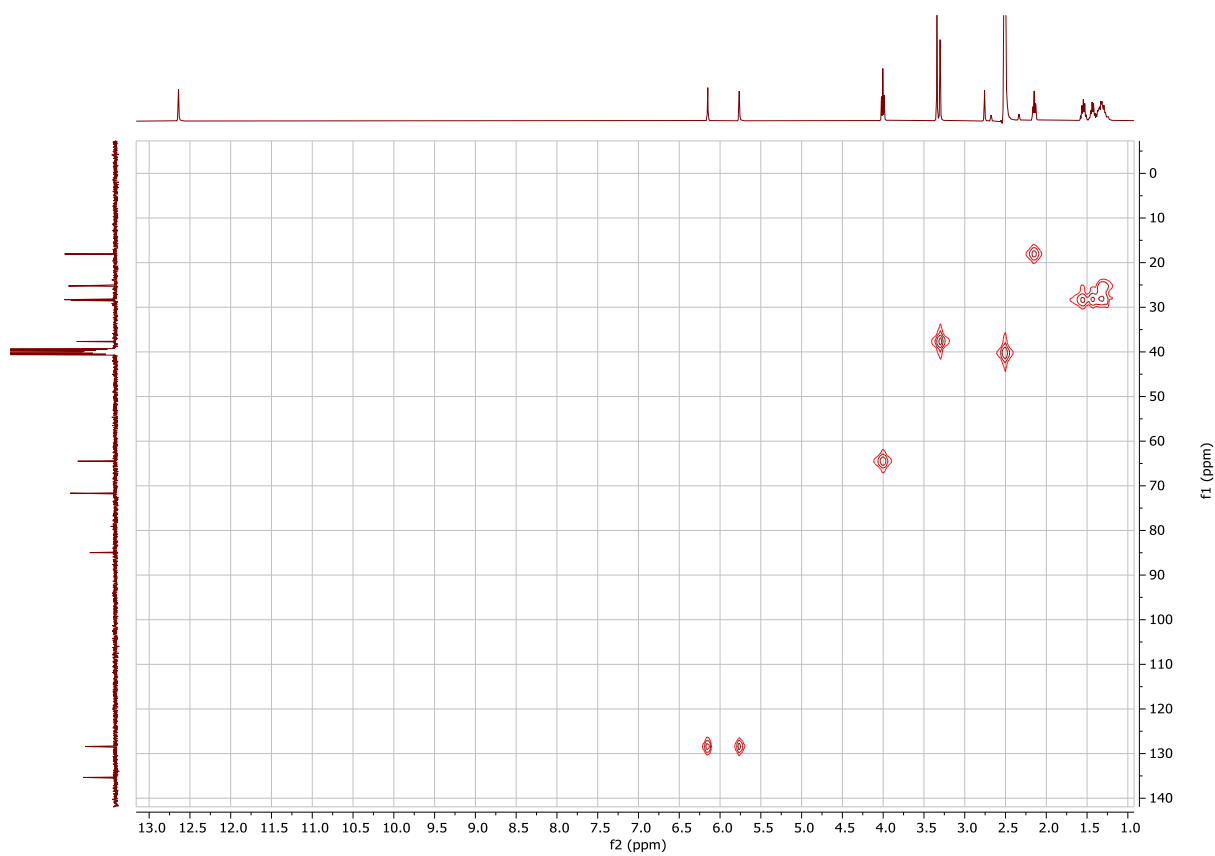


Figure: HSQC NMR spectrum (400/101 MHz, DMSO- d_6) of **4-OI-alk**

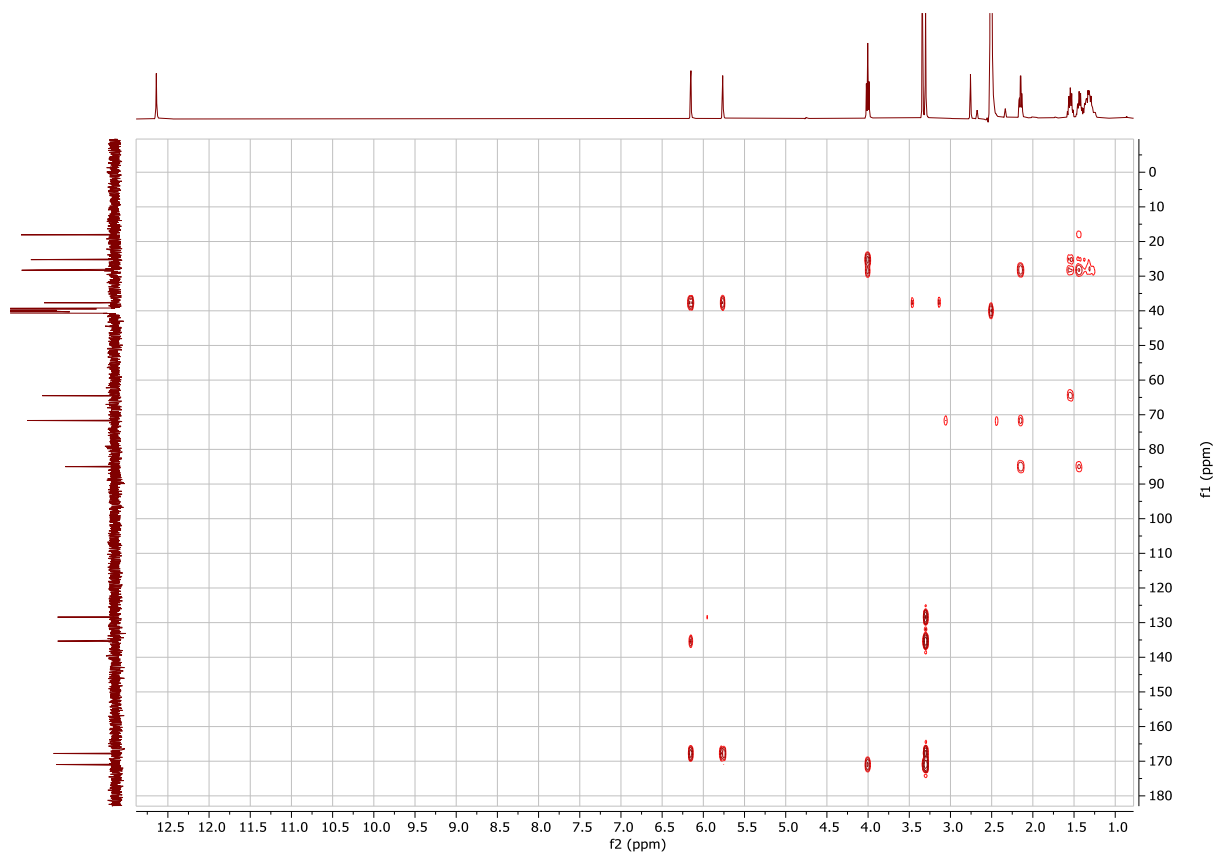


Figure : HMBC NMR spectrum (400/101 MHz, DMSO-*d*₆) of 4-OI-alk

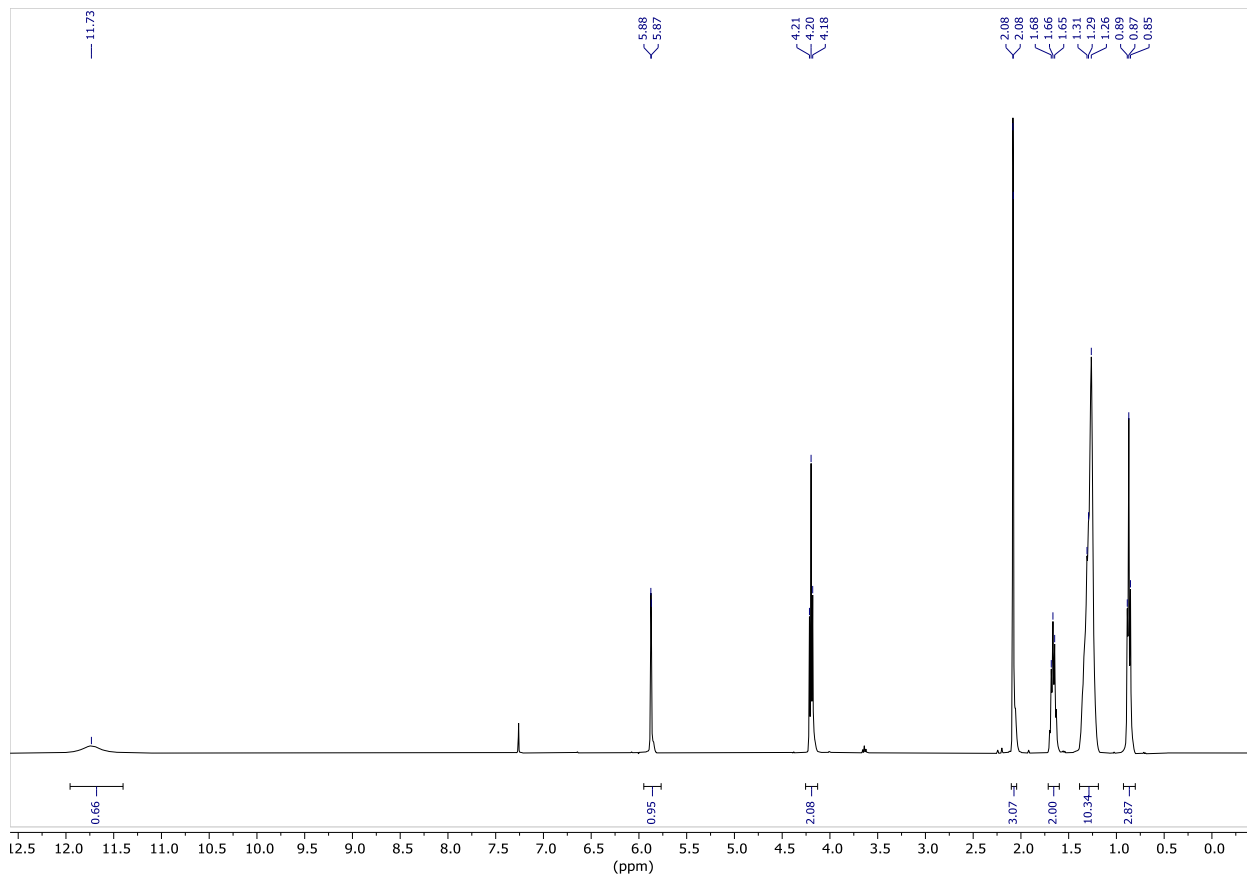


Figure: ¹H NMR spectrum (400 MHz, CDCl₃) of 1-OC (HS)

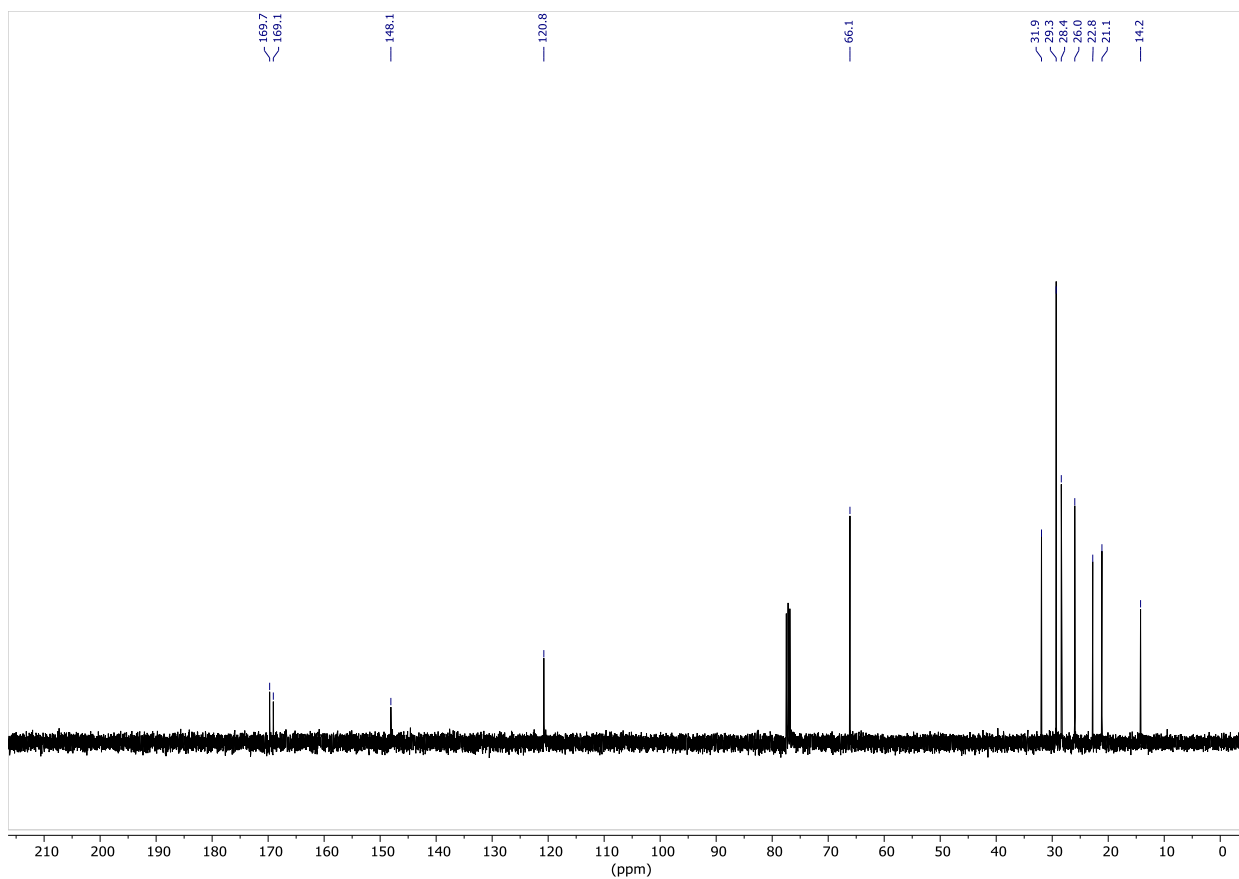


Figure: ¹³C NMR spectrum (101 MHz, CDCl₃) of 1-OC (HS)

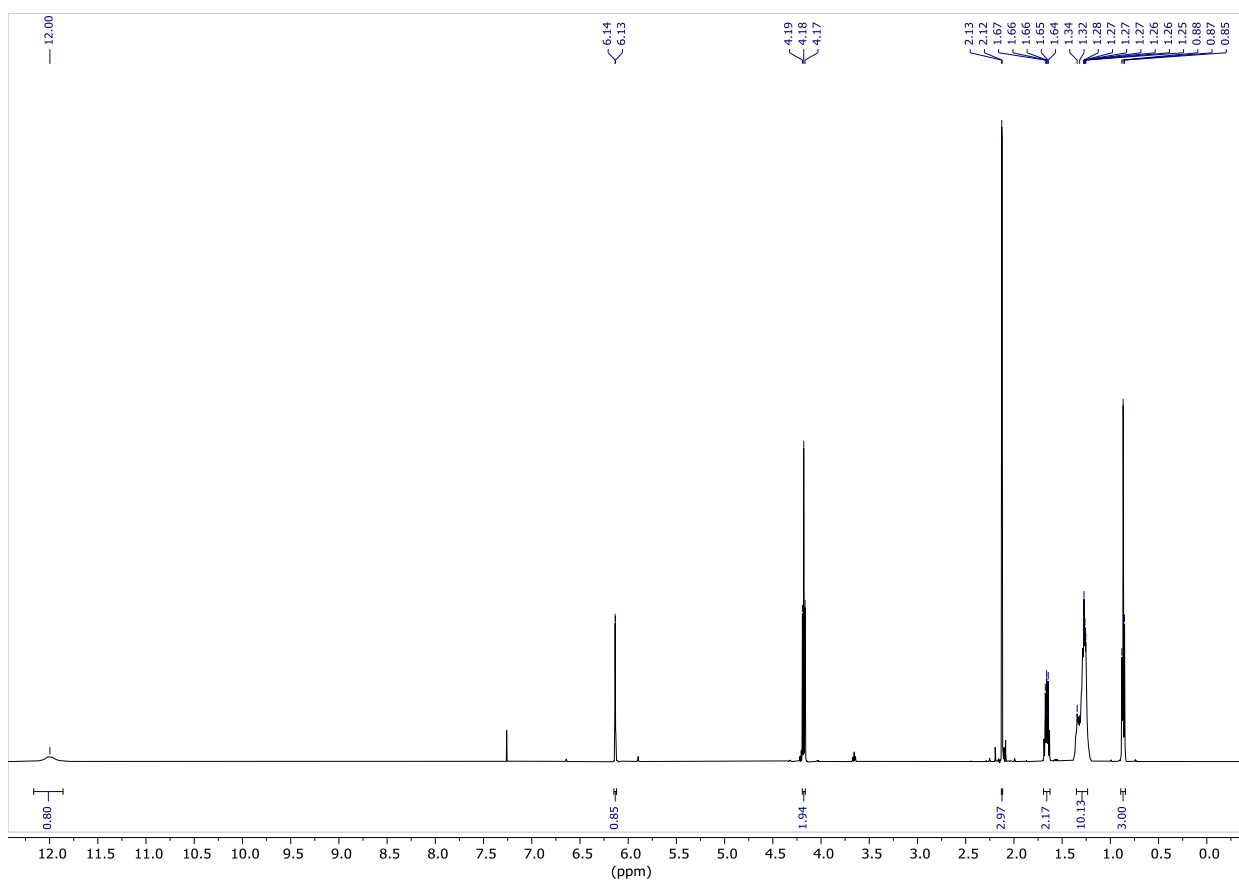


Figure: ¹H NMR spectrum (400 MHz, CDCl₃) of 4-OC (LS)

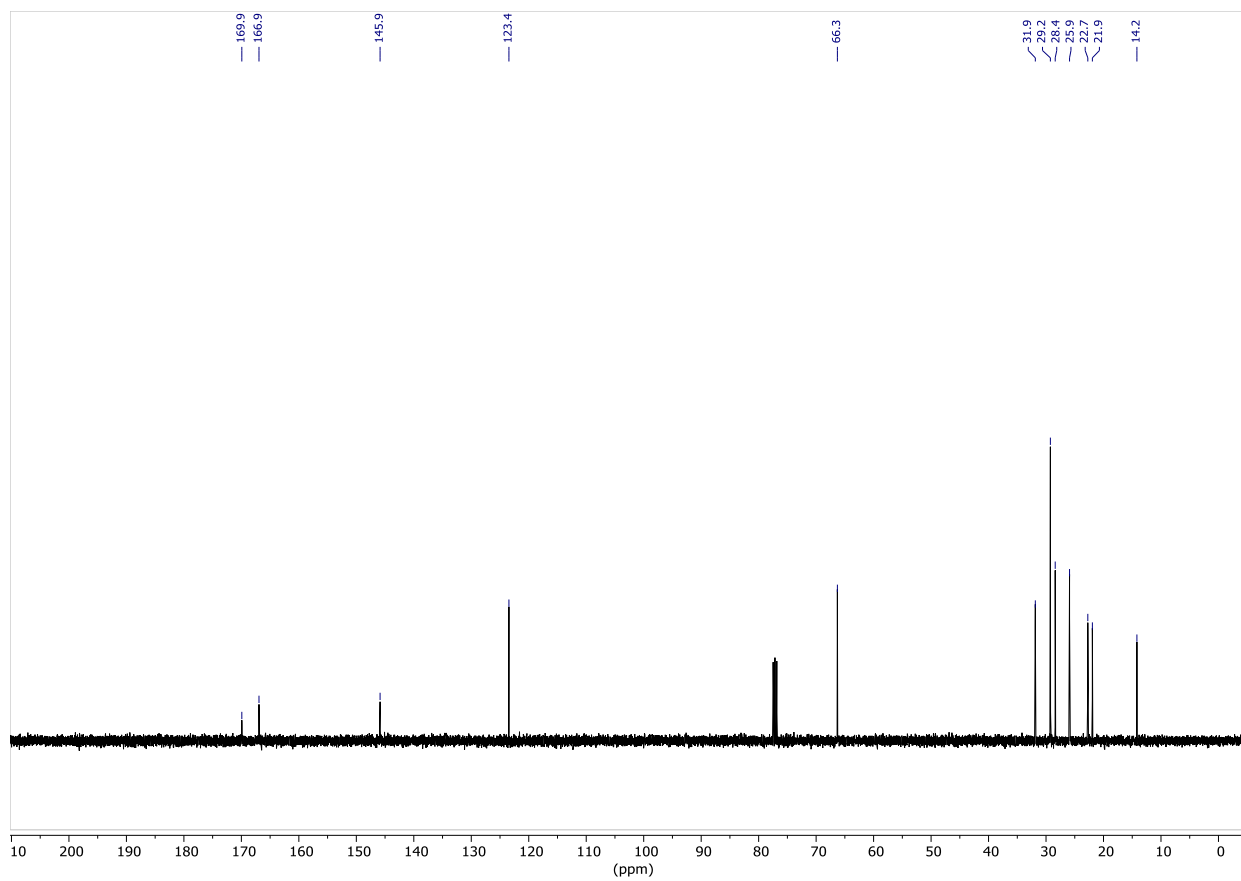


Figure: ^{13}C NMR spectrum (101 MHz, CDCl_3) of 4-OC (HS)